

# Carbon Dot Based Carbon Nanoparticles as Potent Antimicrobial, Antiviral, and Anticancer Agents

Narmin Hamaamin Hussen, Aso Hameed Hasan,\* Yar Muhammed FaqiKhedr, Andrey Bogoyavlenskiy, Ajmal R. Bhat, and Jozaizulfazli Jamalis



Cite This: *ACS Omega* 2024, 9, 9849–9864



Read Online

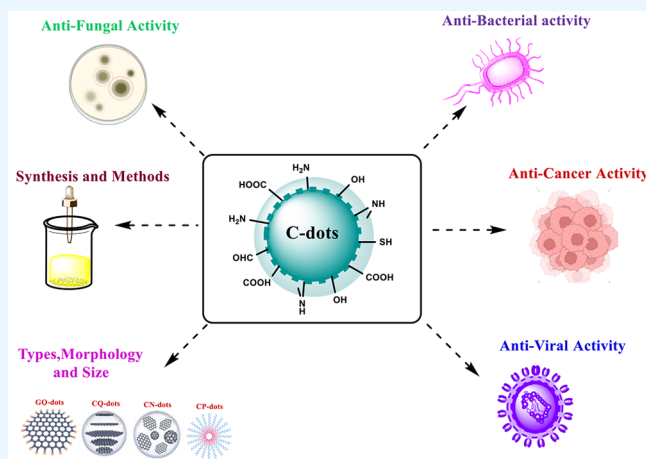
ACCESS |

Metrics & More

Article Recommendations

Supporting Information

**ABSTRACT:** Antimicrobial and anticancer drugs are widely used due to increasing widespread infectious diseases caused by microorganisms such as bacterial, fungal, viral agents, or cancer cells, which are one of the major causes of mortality globally. Nevertheless, several microorganisms developed resistance to antibiotics as a result of genetic changes that have occurred over an extended period. Carbon-based materials, particularly carbon dots (C-dots), are potential candidates for antibacterial and anticancer nanomaterials due to their low toxicity, ease of synthesis and functionalization, high dispersibility in aqueous conditions, and promising biocompatibility. In this Review, the content is divided into four sections. The first section concentrates on C-dot structures, surface functionalization, and morphology. Following that, we summarize C-dot classifications and preparation methods such as arc discharge, laser ablation, electrochemical oxidation, and so on. The antimicrobial applications of C-dots as antibacterial, antifungal, and antiviral agents both in vivo and in vitro are discussed. Finally, we thoroughly examined the anticancer activity



displayed by C-dots.

## INTRODUCTION

Carbon dots (C-dots) are a novel type of carbon-based nanomaterial discovered by Xu et al. in 2004. C-dots were accidentally discovered during the separation and purification of single-walled carbon nanotubes, showing that the carbon size is less than 10 nm.<sup>1</sup> Sun et al. presented a synthetic approach to making C-dots with improved fluorescence emissions via surface passivation in 2006 and termed them carbon quantum dots (CQ-dots), carbon nanoparticles (CNPs), or carbon nanodots (CN-dots).<sup>2</sup> C-dots are studied and are of interest to scientists all over the world compared to 2D carbon materials due to their unique, novel properties, great photostability, ease of production, strong biocompatibility, high quantum yield, small size, low toxicity, low cost, weak interactions with proteins, and good water solubility, providing important applications in many fields including chemistry, engineering, and biological science along with their respective applications, particularly in imaging and therapeutics.<sup>3–5</sup> In the last ten years, the biological and biomedical application of C-dots has become widespread due to their small size (110 nm), unique optical properties, easy functionalization, and bioactivity. Because of their small size, they can cross numerous natural biological barriers in vivo, including ion channels, the blood–brain barrier (BBB), and

the glomerular filtration barrier. Owing to their tunable functional properties, they are suitable nanocapsules and nanocarriers for loading and transporting drugs and genes to specific sites in vivo. In addition, the optical qualities of some C-dots open up possibilities for biomedical applications.<sup>6,7</sup> C-dots exhibit significant absorption in the near-infrared spectral range, which enables in situ photothermal effects in photoacoustic imaging and photothermal therapy. C-dots are also used as fluorescent contrast agents for deep tissue fluorescence imaging.<sup>8–10</sup>

To date, there have been many excellent reviews on the synthesis and chemical and physical properties of C-dots. However, rather than offering a thorough discussion of all of these domains, most of them focus on a single element (synthesis, characteristics, or biological use). Furthermore, the field of C-dots as a whole is rapidly evolving, particularly in biological and biomedical fields. Over the past ten years,

Received: July 29, 2023

Revised: January 26, 2024

Accepted: February 6, 2024

Published: February 22, 2024



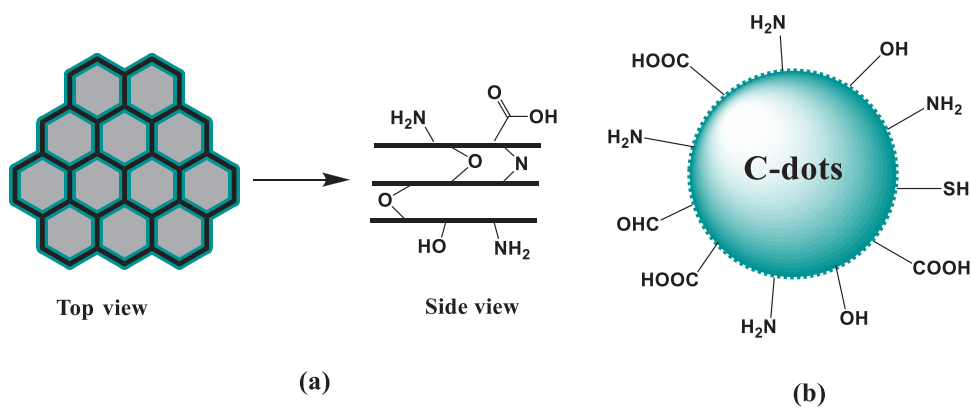


**Figure 1.** Image (a) showcases the top and side views of disk-shaped C-dots. These types of C-dots are composed of sheets that mimic graphene and are connected in a honeycomb form by aromatic carbon rings. (b) Core–shell schematic view of a typical quasi-spherical C-dot structure.

around 40% of all articles published on C-dots have dealt with the bioapplications of C-dots or their composite materials. Regular summaries of recent developments in the application of C-dots in biological and biomedical domains are thus required for charting the field's future orientations, necessitating the publication of regular thorough review papers.<sup>11,12</sup> This Review aims to highlight recent advances using C-dots as a privileged scaffold in medicine, focusing on research articles published in the past 10 years. Several aspects of C-dot use will be summarized, including structure, classification, synthetic methodologies, applications, and biological activities such as antibacterial, antifungal, antiviral, and anticancer.

### ■ STRUCTURE OF C-DOTS

C-dots' application potential is determined by their structure. Carbon materials are extremely well-known, and these include graphite, diamond, fullerenes, carbon nanotubes, and graphene. The size and surface chemical groups of these materials need to be carefully regulated in order to make them bright.<sup>83</sup> The fundamental characteristics of C-dots are always at least one dimension less than 10 nm and fluorescence. A carbogenic core made up of crystalline and amorphous components with surface functional groups is how C-dots are typically explained.<sup>13</sup> C-dots are core–shell structures, according to numerous studies, with no apparent boundary between the carbon core and the polymer shell. Polycrystalline nano-domains containing microscopic carbon clusters are frequently found in the core, which is surrounded by amorphous domains. The conjugated or diamond-like structure of carbon clusters as subdomains in the carbon core can be determined using the transmission electron microscope lattice (TEM). The C-dots have unique characteristics due to the presence of the polymer surface. Atomic force microscopy (AFM) and dynamic light scattering (DLS) can usually detect the polymer side chains.<sup>14</sup> The periodicity of the crystalline graphitic core has been verified by utilization of high-resolution transmission electron microscopy (HRTEM) studies. Rui Zhang et al. used HRTEM to analyze C-dots, which show uniform, monodisperse C-dots with a diameter of  $3.5 \pm 1$  nm. Additionally, they discovered a single C-dot's distinct lattice fringes. The manufactured C-dots are stereoscopic rather than planar like graphene, as indicated by the height along the white line in the AFM, which was utilized to assess the thickness of the material in order to further examine the morphology of C-dots. The created C-dots are oxygen-rich, according to XPS analysis, which was also done to examine the elemental makeup of the C-dots.<sup>15</sup>

A comparison of the particle sizes confirms the presence of side chains. The comparison of the structural parameters of the C-points with the model-adapted small-angle X-ray scattering (SAXS) modes has recently proved the existence of the core–shell structure.<sup>16,17</sup>

### ■ SURFACE FUNCTIONAL GROUPS OF C-DOTS

Depending on the type of precursor, various functional groups such as  $-\text{OH}$ ,  $-\text{COOH}$ ,  $-\text{CHO}$ ,  $-\text{NH}_2$ , and  $-\text{SH}$  can be applied to the surface of C-dots during the manufacturing process. The number and type of functional groups in a system can affect its properties. C-dots with oxygen-containing functional groups are usually negatively charged, while C-dots with N-containing functional groups are positively charged. The charge difference gives C-dots various passivation capabilities. The carboxyl group present on the surface contributes to its aqueous solubility, while other chemical groups facilitate surface functionalization and passivation. Therefore, it is important to know the number of functional groups on the surface of C-dots.<sup>18</sup> The quantity of amino groups is commonly determined using ninhydrin colorimetry in which lysine is used as a standard solution to create a standard curve, and the spectrum of the resulting solution is measured with an ultraviolet spectrometer at 560 nm. Boehm titration can be used to determine the carboxyl group concentration by combining C-dots with  $\text{NaHCO}_3$  solution and then titrating the mixed solution with HCl, with pH as the end point. Wang et al. used normal alkali titration methods to determine the total quantity of hydroxyl and carboxylic acid, followed by conductometric titration to determine the relative content of hydroxyl and a carboxylic acid, and finally computed their respective contents.<sup>19</sup>

### ■ MORPHOLOGY AND SIZE OF C-DOTS

Despite the fact that most C-dots have structures like dots, researchers have used precursor selection and reaction process design to generate C-dots with a wide range of sizes and morphologies (such as triangles, rods, and ribbons).<sup>20</sup> Two main morphologies can be obtained using the term carbon dot. The first is similar to 2D graphene-like sheets made up of 1–3 layers on average which are disk-shaped with surface groups.<sup>21</sup> The more common shape is a more complex structure possessing various tunable surface groups on quasi-spherical polyaromatic crystalline and/or amorphous carbon networks (Figure 1).<sup>22</sup> The majority of morphologies are composed of

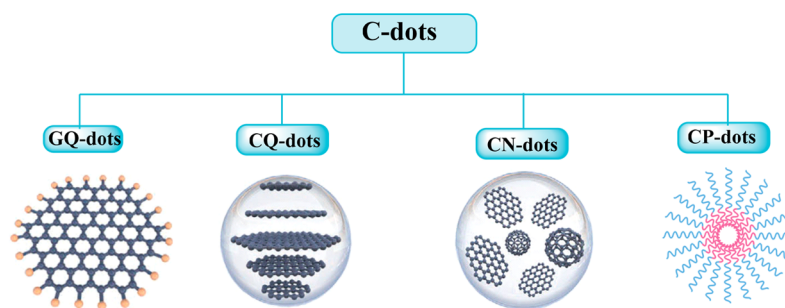


**Figure 2.** Structures of the four different types of C-dots: graphene quantum dots (GQ-dots), carbon quantum dots (CQ-dots), carbon nanodots (CN-dots), and carbonized polymer dots (CP-dots).

**Table 1. Comparison of the Advantages and Disadvantages of Different C-dot Synthesis Methods**

	Synthetic Methods	Advantages	Disadvantages	Refs
Top-down	Laser ablation	Fast, efficient, extremely flexible, easy to set up, and modify the experimental conditions to produce particles with varying sizes and variable shape	Poor control, low yield, and high prices	39,40
	Electrochemical oxidation	Low cost, strong reproducibility, controlled size, high purity, and high yield	Complex process, particularly when heteroatom doping is involved	8
	Ultrasonic synthesis	Easy operation	High energy costs and waste from instruments	31,41
	Arc discharge	Large-scale preparation	Low quantum yield and low purity	21
	Chemical oxidation	Low-cost equipment that can generate C-dots on a large scale	Environmental pollution, harsh procedures, multiple steps, and insufficient size control	42,43
Bottom-up	Hydrothermal treatment	Inexpensive, nontoxic, ecologically friendly, and easy to manage in terms of the reaction vessel's temperature, time, and pressure	Poor control over sizes, long synthesis duration, and low yield	44,45
	Pyrolysis	Easy operation, solvent-free, low-cost, and large-scale production	Nonuniform size distribution	46,47
	Microwave synthesis	Fast, inexpensive, eco-friendly, and is easy to control the size of the particles, with the C-dots produced being uniform in size distribution	Poor control over size, high energy cost	35,36
	Solvothermal	Inexpensive, eco-friendly, nontoxic	Poor control over sizes	48,49
	Thermal decomposition	Easy operation, solvent-free, low cost, and can produce C-dots at a large scale	Low yield	50,51

carbon atoms because of organic or pure carbon precursors, with the addition of oxygen, nitrogen, and possibly more dopants based on the elements in the starting materials and the reaction conditions, including time and temperature, as hypothesized. The produced C-dots have a unique triangular shape because of the presence of three highly active hydrogen atoms at three meta locations in the symmetrical precursor phenolglucinol. Three electron-donating hydroxyl groups in a single molecule activate it. To regulate the size of CDs, a suitable quantity of concentrated sulfuric acid was introduced to the ethanol solution acting as a catalyst. As size increases, the emission wavelength red shifts, as expected by quantum confinement effects.<sup>23</sup>

In one study, researchers observed the effect of changing the reaction atmosphere, and the result was C-dots of different properties yielded by each of the tested gases, with aromatization production in the highest degree in oxygen.<sup>24</sup>

## ■ CLASSIFICATION OF C-DOTS

Graphene quantum dots (GQ-dots), CQ-dots, CN-dots, and carbonized polymer dots (CP-dots) are examples of the different types of nanosized fluorescent carbon materials collectively referred to as C-dots. These materials are categorized according to their unique carbon core structures, surface groups, and properties as shown in Figure 2.<sup>25</sup> The GQ-dots are small graphene fragments composed of single or few graphene layers with obvious graphene lattices and

chemical groups at the edge or inside the interlayer defect that contribute to unique properties like quantum confinement effect and edge effect. They typically have side dimensions that are anisotropic, less than 20 nm, and a height that is fewer than five layers of graphene ( $\approx 2.5$  nm).<sup>26</sup> The CQ-dots are always spherical and have apparent crystal lattices and chemical groups on the surface, showing intrinsic state luminescence and a quantum confinement effect of the CQ-dot size. It is of great importance to control the photoluminescence wavelength by tuning the CQ-dot size.<sup>27</sup>

The carbonization of CN-dots is postulated to be to a large degree along with some chemical groups on the surface. However, the crystal lattice structure and polymeric properties are oftentimes ambiguous, and the absence of a quantum confinement effect due to particle size in the subdomain state situated inside the graphitic carbon core and defect/surface state give rise to photoluminescence.<sup>28</sup> The CP-dots are known to possess either a hybrid polymer or carbon structure with many surfaces' functional groups/polymer chains and a carbon core. The carbon core can be divided into four subclasses: among them are two types of fully carbonized cores that are on par with CN-dots or CQ-dots, and clusters of tiny carbons encased in a polymer shell come together to create a paracrystalline carbon structure, a highly dehydrated cross-link, and a polymer framework that is tightly knit.<sup>29,30</sup>

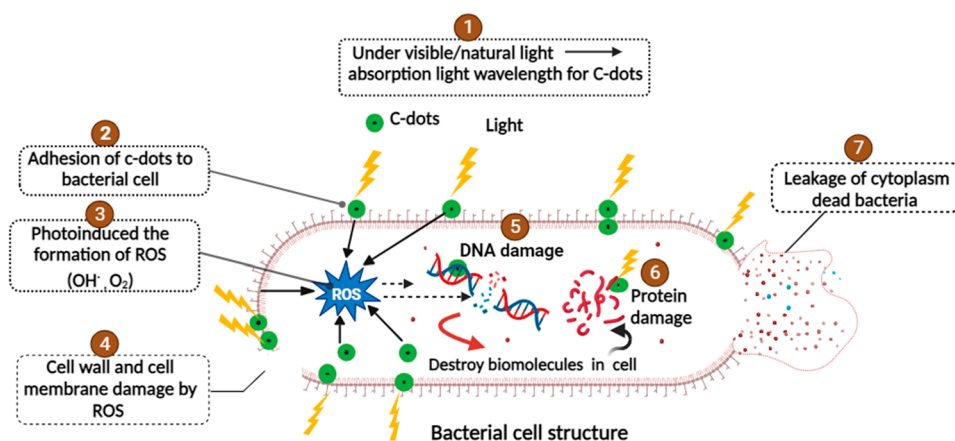


**Figure 3.** Mechanism of action of C-dots' photoinduced antibacterial activity.

## METHODS OF SYNTHESIS OF C-DOTS

The constituents of carbon dots may vary moderately depending on the various synthetic procedures. The significant advancements of C-dots in the past years are evident in the synthesis, characteristics, and applications.<sup>31</sup> Variations in fluorescence, size, and activity are the consequences of synthetic change. Photoluminescence, which is the most well-studied property of C-dots, after conjugation with the desired chemical, allows for simple characterization. The typical spectral emissions of C-dots range from the middle of the 300 nm band to as high as 700 nm. There are two basic ways to synthesize C-dots: (i) the top-down and (ii) bottom-up approach, as shown in Table 1. The processes of top-down larger carbon structures (also known as disassembling), such as graphite, carbon nanotubes, graphite columns, and graphene, are made into smaller carbon structures using laser ablation, chemical oxidation arc discharge, electrochemical oxidation, and ultrasonic methods with a size below 10 nm. Nonetheless, the limitations of the top-down technique include the requirement of expensive ingredients and instruments, strict reaction conditions, and lengthy reaction times.<sup>32–34</sup> The bottom-up (assembling) strategy, however, refers to the formation of suitable sized C-dots from combining smaller carbon bottom-up structures (e. g., citric acid, glucose, phenylenediamine, urea, and fruit juice). The techniques used for the bottom-up method for forming C-dots involve solvothermal processing, microwave synthesis, thermal decomposition, pyrolysis, carbonization, and hydrothermal treatment. Customarily, prior to additional purification processes such as centrifugation, dialysis, electrophoresis, or other separation methods, nitric acid (HNO<sub>3</sub>) is used to oxidize the surfaces.<sup>35,36</sup> Three common potential setbacks in C-dot production require the utmost consideration: (1) Nanomaterial formation would be prevented due to the larger clusters, causing aggregates. Electrochemical synthesis, coordinated pyrolysis, or solution chemistry can prevent this problem. (2) Dimension is a strong influencer for chemical properties and luminescence; therefore, it is best to avoid excessive heterogeneity of size. (3) Production of materials with a myriad of qualities including solubility, photoluminescence (PL), and quantum yield (QY) is made possible by manipulating circumstances of the synthesis and the postsynthesis treatment.<sup>37,38</sup>

## BIOLOGICAL ACTIVITY OF C-DOTS

**Antimicrobial Activity of C-dots.** The ongoing growth of the human population has contributed to pollution of the air and water, which has led to the development of infectious diseases and viruses. One of the main causes of death worldwide is infectious disease, which is brought on by microorganisms such as bacteria, fungi, viruses, or parasites. If the infections continue to evolve into multidrug-resistant (MDR) organisms, many of these diseases will become more difficult to treat, leading to increasing mortality rates and expenditures associated with healthcare.<sup>52–54</sup> Many microorganisms have developed drug resistance over the past few decades as a result of the widespread use of antibiotics, including lactam antibiotics, trimethoprim, fluoroquinolones, carbapenem, and chloramphenicol. Additionally, the epidemiology of resistance has been shown to exhibit substantial variation; the problems associated with resistance are no longer exclusive to certain pathogenic species or select healthcare facilities. Rather, they affect a wide range of major pathogens and many epidemiological settings. This includes acute-care hospitals, long-term care institutions, communities, and others.<sup>55,56</sup> MDR bacterial infections, especially those that result from Gram-positive bacteria, have displayed rapid growth and developed resistance to almost all available antibacterial drugs in the present pharmaceutical market. For instance, the United States Centers for Disease Control and Prevention (CDC) have classified drug-resistant *Streptococcus pneumoniae*, methicillin-resistant *Staphylococcus aureus* (MRSA), and *Enterococcus faecalis* (VRE) as severe public health problems.<sup>57</sup>

Globally, there are significant issues due to the rise in MDR caused by microorganisms and the continuous decrease in the development and finding of novel antibiotics. According to projections, the spread of antibiotic resistance by 2050 might result in 300 million more deaths and cost an additional US \$100 trillion, necessitating immediate and effective action to address the MDR problem. There are several different disinfectants and antiseptics that are used for the inactivation of pathogenic bacteria and infection control regularly used in hospitals and other healthcare units. Limitations of the majority of these agents are excessive toxicity and irritation, resulting in unwanted effects such as contact dermatitis and mucous membrane irritation, and pathogenic resistance and adaptability cause loss of efficacy in some of them.<sup>58,59</sup>

Therefore, in an effort to fight MDR, the current situation necessitates immediate action toward the development and discovery of new antimicrobial strategies and agents that possess enhanced efficacy and reduced toxicity. This is crucial for successfully dealing with the issues relating to infection prevention and treatment.<sup>60</sup> Antimicrobial nanoparticles have received a lot of attention as an alternative to antibiotics because of their beneficial qualities and distinctive modes of action against microorganisms. Through intricate mechanisms, they prevent bacteria from developing drug resistance and killing cells, while significant health issues related to biocompatibility still exist for practical usage. The simplicity of synthesis and functionalization, high dispersibility in aqueous media, and potential for biocompatibility make carbon-based materials, particularly C-dots, interesting candidates among the different antibacterial nanomaterials.<sup>61,62</sup>

**Antibacterial Mechanism and Factors Affecting the Antibacterial Activity of C-dots.** The general consensus is that C-dots are both in vitro and in vivo benign and harmless. Through complex processes such as the production of reactive oxygen species (ROS), destruction of cell structure, fragmentation, and condensation of genomic DNA, C-dots prevent the development of bacteria or kill bacteria, causing the cytoplasm to leak. The surface charge and production of ROS can have a significant impact on the antibacterial capacity of C-dots.<sup>63</sup> The production of ROS conveys the main mechanism of the antibacterial property of C-dots, as narrated by the outcome of recent studies. The antibacterial photodynamic therapy's mode of action is illustrated in Figure 3. Light-activated bacterial elimination is one of the safest and most successful approaches. The wavelength at which C-dots absorb light ranges from near UV to visible to near-IR. These include the adherence of C-dots to the surface of bacteria, ROS generated during photoinduction, and ROS that come into contact with the bacterial cell when exposed to visible or natural light. The following occurrences include bacterial cell wall/membrane damage and penetration, morphological changes of the cell membrane, oxidative-stress-induced DNA/RNA damage, expressions of important genes that inhibit or alterations, and the induction of oxidative damage in proteins. This causes damage to certain significant biomolecules in the cell and cytoplasmic leakage causing cell death, by the action of hydroxyl free radicals ( $\text{OH}\bullet$ ) and/or singlet oxygen ( $^1\text{O}_2$ ) production.<sup>64,65</sup> ROS are notorious compounds/atoms known to cause irreversible protein inactivation intracellularly, peroxidation of lipids, mitochondrial impairment, and gradual deterioration of the cell membrane, leading to necrosis/apoptosis and ultimately cell death. The process of detoxifying the radical species is complex, and bacteria find it difficult to resist this alternative antibacterial action. According to general expectations, a number of factors, such as surface functionalities, optical properties and photoexcited state characteristics, and of C-dots, influence their antibacterial activities.<sup>66,67</sup> These dependencies present opportunities to modify and improve the bactericidal effects of C-dots activated by visible or ambient light. The existing experimental findings have demonstrated significant potential for C-dots as a novel category of potent antibacterial agents that can be readily activated by visible or natural light. Nevertheless, a comprehensive understanding of the mechanisms underlying the generation of ROS by a variety of C-dots and the resulting antibacterial activities remains to be elucidated.<sup>68</sup>

As mentioned previously, C-dots possess a variety of antibacterial actions and factors affecting the antibacterial activity of C-dots including the following.

**Charge on C-dots.** C-dot interactions with cell membranes of bacteria are largely impacted by their type and degree of charge. Being et al. reported that bacterial cell wall interactions are different for the synthesis of positively, negatively, and neutrally charged C-dots obtained from spermine, candle soot, and glucose, respectively. The positively charged C-dots are concluded to be antibacterial; bacteriostatic action is noted from negatively charged C-dots and neutral C-dots. However, they are hardly active against *E. coli*. Furthermore, positively charged C-dots are observed to produce more ROS than negatively charged C-dots, while neutral C-dots produce very little ROS. Nevertheless, no direct relationship between surface charge and ROS formation has been discerned.<sup>68</sup>

**Shape and Size of C-dots.** Su et al. illustrated how the shape and source material of C-dots influence their antibacterial activity. Su et al. found that GQ-dots had size-dependent antibacterial action against *E. coli*. Because of their tiny size at 15 nm, small-lateral-sized GQ-dots may readily penetrate the plasma membrane, causing higher oxidative stress and membrane rupture in comparison to large-lateral-sized GQ-dots at 50 nm. ROS production mediated by these GQ-dots has been linked to membrane breakdown and oxidative stress.<sup>69</sup>

**Functional Groups on C-dots.** C-dot functional groups have a significant impact on antibacterial activities. As an instance, the utilization of amine-functionalized C-dots that were modified with lauryl betaine has been shown to possess dual characteristics of antibacterial activity and bacterial distinction. This leads to the selective fluorescence labeling and eradication of Gram-positive bacteria while coexisting with both Gram-positive and Gram-negative bacteria. By selectively adhering to Gram-positive bacteria, positively charged quaternized C-dots with a lengthy and multicolor fluorescence emission may distinguish between Gram-positive (*S. aureus*) and Gram-negative (*E. coli*). Furthermore, the quaternized C-dots' minimum inhibitory concentration (MIC) for *S. aureus* may be considerably lowered, reaching as low as  $8 \text{ mg mL}^{-1}$ . Because the C-dots include both hydrophobic hydrocarbon chains and positively charged quaternary ammonium groups, they may be selectively attached to Gram-positive bacteria for differentiation and suppression. After 2.5 h of incubation with the quaternized C-dots, the cell surfaces of *S. aureus* became injured and wrinkled, and intracellular contents seeped out.<sup>70</sup>

Results from several later investigations of C-dots from various syntheses were in agreement with those previously mentioned. As an illustration, Li et al. created C-dots using a one-step electrochemical process with vitamin C as a precursor and discovered that they have broad-spectrum antibacterial activity against *S. aureus*, *B. subtilis*, *Bacillus sp.* WL-6 variant of *B. subtilis*, *E. coli*, and the ampicillin-resistant *E. coli*.<sup>71</sup> The inhibition of growth of *B. subtilis* and *Bacillus sp.* WL-6 cells by a dose of  $50 \text{ }\mu\text{g/mL}$  of the C-dots is achieved. In order to manufacture C-dots using hydrothermal processing at  $200 \text{ }^\circ\text{C}$ , ciprofloxacin hydrochloride, an antibiotic, was used as a precursor by Hou et al.<sup>72</sup> The stated goal of the moderate processing conditions was to maintain some ciprofloxacin-like structure on the dot surface. The MIC value of the dot sample exhibited a lower value for *E. coli* in comparison to *S. aureus*, indicating that the sample had less antibacterial efficacy against Gram-positive than Gram-negative bacteria. At a relatively low

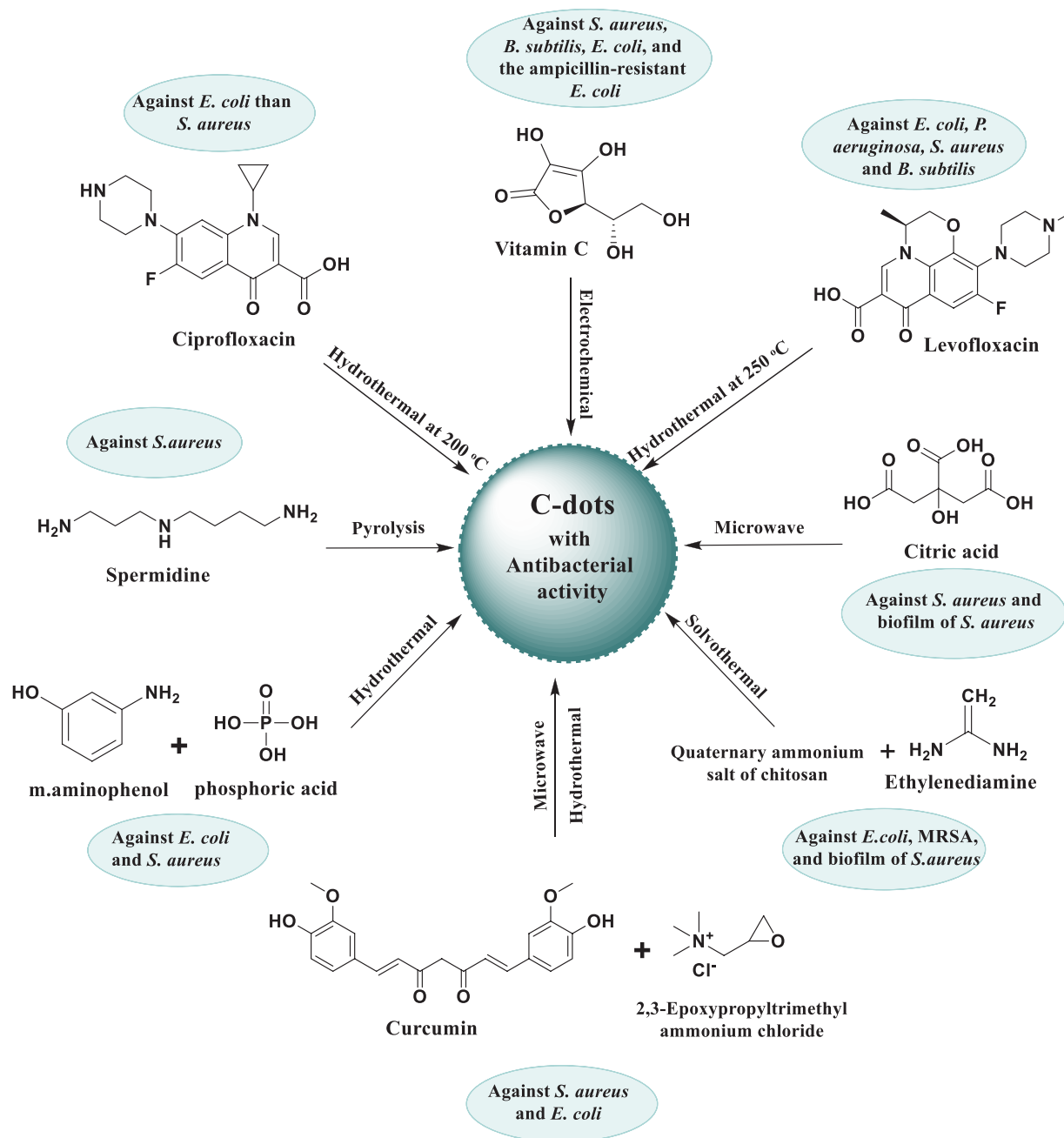


**Figure 4.** Sources of C-dots and their broad-spectrum antimicrobial activity against Gram-positive and Gram-negative bacteria.

temperature of only 120 °C, penicillin was also employed as a precursor for C-dots in a similar hydrothermal carbonization technique.<sup>73</sup>

A one-step hydrothermal process was carried out by Liang et al. in order to use Levofloxacin hydrochloride as a basis for the biosynthesis of novel, broad-spectrum, antibacterial C-dots (named F-C-dots), effectively eradicating both Gram-positive and Gram-negative bacteria in specific toxicity while maintaining a somewhat benign action in mammalian cells. The levofloxacin hydrochloride provided both carbon and fluorine to F-C-dots. Multiple characterization techniques were utilized to determine the structure and morphology of F-C-dots. Spherical F-C-dots are shown to be dispersed uniformly with the absence of aggregates on the transmission electron microscope (TEM), with a crystalline lattice made up of 0.21 nm gaps, as revealed from the HRTEM inset picture,

corresponding the graphitic carbon's (002) plane. By depending on the histogram of size distribution, 1.27 nm is dictated to be the average particle size of F-C-dots. The height of F-C-dots is nearly 2 nm on the basis of the AFM, F-C-dots. Smaller sized C-dots possess more antibacterial activity due to their interaction with DNA molecules and cellular absorption. Mechanistic bacterial cell wall/outer membrane interruption is made possible for F-C-dots through their point-to-plane contact interaction, miniscule size, and excellent aqueous solubility. The antibacterial activity that depended on time and concentration was studied. Additionally, the processes of ROS production and bacterial morphology were the main hopeful outcome for the investigation of antibacterial activity of F-C-dots. It is important to note that F-C-dots can act as ideal photocatalysts with no need for light for ROS production; therefore, the light-irradiated disinfection's prolonged exposure

time is reduced. Synthesis of novel and potent nanoantibiotics will stem from further research in the field of antibacterial processes and the synergistic antibacterial mechanism.<sup>74</sup>

Paulina et al. carried out the study of the citric-acid-based antibacterial photodynamic effect of C-dots synthesized from a single-pot microwave-assisted technique, both *in vitro* and *in vivo*. The efficacy of photoilluminated C-dots (combination of C-dots and light) against *S. aureus* suspensions and biofilms was evaluated by *in vitro* tests. C-dot concentrations of 6.9 and 13.8 mg/mL as well as lighter doses of 20 and 40 J/cm<sup>2</sup> were shown to greatly eradicate the bacteria. Based on these factors and the outcomes, mice were used in *in vivo* tests to assess the efficacy of this treatment on *S. aureus*-infected wounds. According to the viability test, the bacteria on the skin lesions were reduced by 104 log due to C-dot-mediated photodynamic inactivation. These findings collectively demonstrated that Gram-positive bacteria-infected wounds can be successfully treated with antibacterial photodynamic therapy employing C-dots.<sup>75</sup> Hong-Jyuan et al. found enhanced bacterial keratitis in relation to spermidine (Spd) powder. Spermidine trihydrochloride powder was directly pyrolyzed to create supercationic C-dots (C-dots pds). Gram-positive and Gram-negative bacteria, as well as multidrug-resistant pathogens like methicillin-resistant *S. aureus*, were all successfully eradicated by the C-dots pds (MRSA) (Figure 4). A strong positive charge was thought to be the cause of the C-dots pds' antibacterial effect because it severely disrupted bacterial membranes and killed them. Ocular infusion of C-dots pds can cause the tight junction of corneal epithelial cells to open and treat an infection brought on by *S. aureus*, based on *in vivo* antibacterial study in the treatment of BK in rabbit eyes.<sup>76</sup>

According to Chai et al., P-doped C-dots can be made from *m*-aminophenol and phosphoric acid via a straightforward hydrothermal process in which fluorescence is emitted at 501 nm when the combined compound is excited at 429 nm. P-doped C-dots are effective combatants of both *Escherichia coli* (*E. coli*) and *Staphylococcus* (*S. aureus*). The minimum inhibitory concentration (MIC) of P-doped carbon dots is 1.23 and 1.44 mg/mL in *E. coli* and *S. aureus*, respectively. Moreover, the effects observed during exposure to the P-doped C-dots and morphological injury were developed in *E. coli* cells, and abnormalities were noted in *S. aureus*. Zeta potential research showed that the P-doped C-dots interfere with antibacterial activity and break down bacterial structure through electrical interaction. The findings of this research show that the P-doped C-dots as prepared can be a promising therapy option for bacterial infections.<sup>77</sup> Additionally, according to a recent study by Zhao et al., several antimicrobial effects were observed in C-dots synthesized from quaternary ammonium salt of chitosan (QCS) and ethylenediamine (EDA), the mechanism of which is speculated to be by rupturing membranes, damaging DNA and proteins, and producing singlet oxygen. With a minimum inhibitory concentration of 10 µg/mL, both Gram-positive and Gram-negative bacteria are shown to be susceptible to the C-dot's outstanding broad-spectrum inhibitory activity against them, predominantly the *Staphylococcus aureus* biofilm samples, demonstrating their great potential for eradicating bacteria and biofilms. According to the results of the biocompatibility tests, QCS-EDA-C-dots show minimal hemolytic effects and are not harmful to human normal hepatocytes. Additionally, due to the manufactured QCS-EDA-C-dots superior optical qualities, their use is successfully demonstrated in the imaging

of biofilm and bacteria.<sup>78</sup> Wu et al. applied a "double-thermal" approach to create curcumin-quaternized carbon quantum dots with good solubility and stability. They next tested the antibacterial effectiveness of the materials using the disk diffusion and broth dilution methods. It is suggested that the active curcumin and quaternary ammonium groups on the surfaces of Q-C-dots would still be present to increase the antibacterial activity. Based on scientific research, it has been shown that Q-C-dots exhibit a notable and extensive antibacterial efficacy, surpassing the inherent antibacterial properties of natural curcumin. The antibacterial mechanism of Q-C-dots was examined, and it was discovered that Q-C-dots functionalized with  $-N^+(CH_3)_3$  had strong adhesion to bacterial cell membranes. The bacterial cells became compromised, much like a "Trojan Horse", and the Q-C-dot entrance led to the production of ROS and the efflux of cytoplasmic DNA and RNA, which ultimately caused the death of the bacteria. The bacterial resistance of Q-C-dots was not seen, and neither hemolysis nor cytotoxicity were caused by Q-C-dots. The *S. aureus*, *E. coli*, and mixed bacterial infection wound healing experiments with a mice model showed that Q-C-dots reduced the bacterial population at the wound site, lowered inflammation, and improved wound healing *in vivo*. These results showed that the Q-C-dots would be a promising antibacterial candidate for treatments such as bacterial resistance to infections and infected wound healing.<sup>79</sup>

**Antifungal Activity of C-dots.** The antifungal activities of C-dots have been the subject of several studies. Li et al. discovered that the C-dots designed for bacteria inactivation additionally displayed extensive antifungal properties toward *R. solani* and *P. grisea*.<sup>71</sup> The antifungal properties of C-dots and their derived conjugates against the fungus *C. albicans* were investigated by Priyadarshini et al.<sup>80</sup> Additionally, C-dots have antifungal properties on *Candida albicans*, according to Jhonsi et al.<sup>81</sup> Similar to that, *Saccharomyces cerevisiae* yeast cells were another sample to have C-dots conjugated with ciprofloxacin tested on them, and brilliant fluorescence emissions of green color were believed to be caused by the C-dots inside the cells. Curiously, in their investigation, Rispail and co-workers conducted an experiment involving the combination of nanoscale carbon with ZnS. The researchers observed that the resultant nanostructures could be extensively absorbed by the hypha of the *Fusarium oxysporum* fungus. However, it was found that these nanostructures showed no toxicity toward the fungus.<sup>82</sup> On the other hand, in a study that has been described by Bagheri et al., the treatment with C-dots was used to prevent the growth of yeast cells (*Pichia pastoris* X33 wild type), which was accompanied by noticeably altered yeast cell shape.<sup>83</sup> In a more recent study, Kaloyan et al. looked into how differing C-dot concentrations affected the growth of three significant plant pathogens: *Botrytis cinerea*, *Alternaria alternata*, and *Fusarium oxysporum*. They calculated the range of this impact and discovered that *P. infestans* growth slows down as C-dot concentration rises. Therefore, 10 g/mL of subinhibitory C-dots was chosen and employed to treat sporangia along with gene-specific dsRNA. Here, the C-dot inhibitory effect against a number of plant diseases as well as their capacity to improve RNAi in *P. infestans* was shown. Low toxicity toward human cells was also shown.<sup>84</sup>

**Antiviral Activity of C-dots.** The four main stages of virus infection must be completed: attachment, penetration, replication, and budding. The C-dots are able to stop viral infections at various stages by thwarting viral attachment,

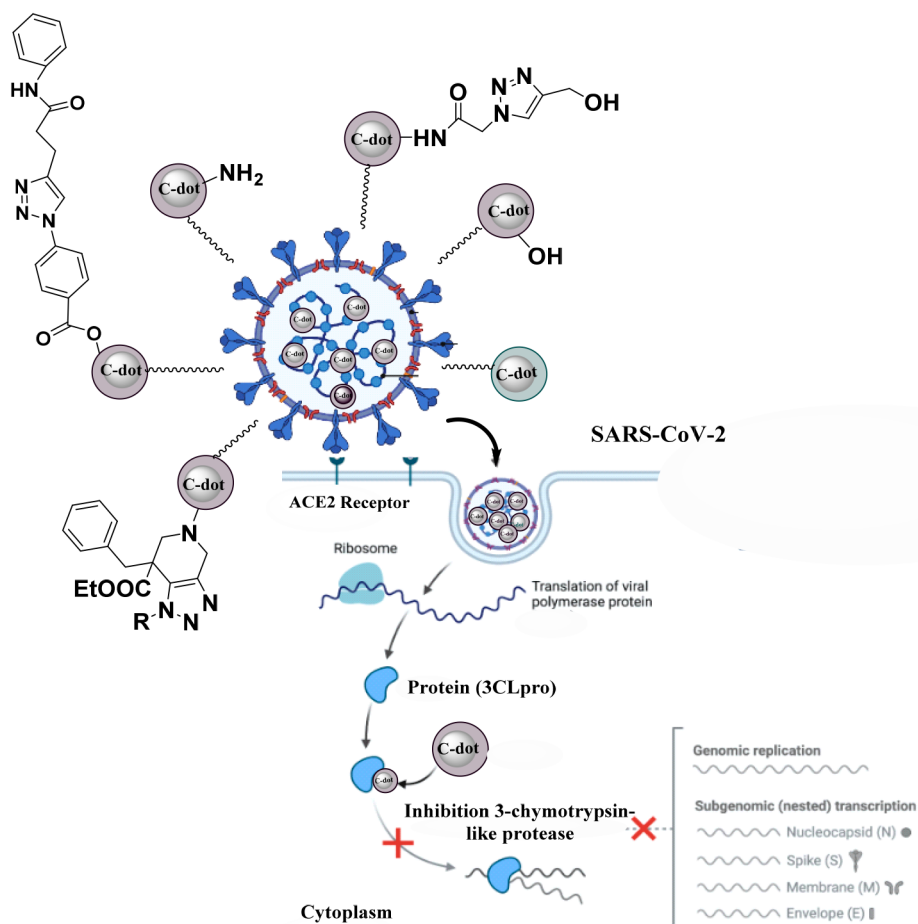


**Figure 5.** Potentially generated triazole-based carbon dots that are resistant to SARS-CoV-2 infection and replication enzymes like helicase and 3-chymotrypsin-like protease (3CLpro) are blocked, ultimately inhibiting human coronavirus.

preventing viral penetration, interfering with viral replication, and halting viral budding. For a cell to become infected, the virus must connect to it and penetrate it. The virus will be successfully rendered inactive by blocking the first two phases.<sup>85–88</sup>

Recently, Huang et al. discovered that flaviviruses (such as Japanese encephalitis, Zika, and dengue causing viruses) and nonenveloped viruses (such as porcine parvovirus and a virus associated with adenovirus) could become a lethal infection and get prophylaxis from C-dots produced from the benzoxazine monomer in vitro. This was most likely accomplished by directly binding to the virion's surface and subsequently preventing the first stage.<sup>89</sup>

In 2020, Hai-Ting et al. discovered that the polyamine C-dot viral infection prophylactic effect comes from C-dots adhering to the envelope of the White Spot Syndrome Virus (WSSV) with dosage-dependent inhibitory effects. Cryo-electron microscopy revealed that the virus treated with polyamine C-dots had a higher number of polyamine C-dots adhering to its envelope than the control group did. The death rates were then much lower than those of the control group when the WSSV-infected shrimp were fed a feed containing polyamine C-dots. These results showed that C-dots could prevent shrimp from becoming infected with WSSV, increasing their chances of surviving. Since the virus envelop structure was damaged and its penetration was prevented, this C-dot antiviral mechanism is thought to have prevented infection. Actually, C-

dots can interact with the viral envelope or a component of the host cell to prevent the virus from adhering and from penetrating.<sup>90</sup> Garg et al. have described the inhibitory mechanism of human coronaviruses by heteroatom-doped carbon dots in their research. The study team suggests that a variety of bioisosteres be used to potentially generate triazole-based carbon dots that are resistant to severe acute respiratory syndrome coronavirus 2 (SARS-CoV-2) infection (Figure 5). The numerous hydrophilic functional groups on the edges of carbon dots make them suitable for a variety of biomedical applications. Additionally, in order to optimize the level of virus contact, these magical nanomaterials' surface functioning is crucial.<sup>91</sup>

According to a study by Barras et al., herpes simplex virus type 1 (HSV type 1) infection could be prevented by the surface-functionalized (addition of functional groups) capability of C-dots. The spread of virus in HSV type 1 infected A549 and Vero cells is made possible effectively by 4-aminophenyl boronic acid hydrochloride used to synthesize the C-dots. Depending on the study, carbon dots prevent viral entrance to the host cell.<sup>92</sup> The most efficient methods for preventing infection after a virus reaches a host cell are to stop replication and prevent budding. Coronavirus infection can be effectively prevented using cationic carbon dots made of curcumin. Curcumin and citric acid were combined hydrothermally in an autoclave coated with Teflon to create curcumin carbon dots, which were subsequently purified by

**Table 2. Precursor, Virus Species, and Antiviral Activity of C-dot Formation**

Precursor to the synthesis of C-dots	Virus species	Mechanism of antiviral activity	Ref
Monomer of benzoxazine	Parvovirus in pigs, adenovirus-associated virus, Zika and Dengue fever virus, and Japanese encephalitis	First stage of virus-host cell interaction is blocked by the C-dots directly connecting to the surface of the virus.	89
Polyamine	Whispovirus including WSSV	C-dots can interact with the White Spot Syndrome Virus (WSSV) envelope or a component of the host cell to prevent the virus from adhering and from penetrating	90
Triazole derivatives	Severe acute respiratory syndrome coronavirus2 (SARS-CoV-2) among other human coronaviruses	Signification viral replication enzymes like helicase and 3-chymotrypsin-like protease (3CLpro) are blocked ultimately inhibiting human coronavirus	91
4-Aminophenyl boronic acid hydrochloride	Type 1 herpes simplex virus (HSV)	C- dots prevent the herpes simplex virus from entering the host cell	92
Curcumin and citric acid	Coronavirus	Suppression of viral replication by mechanisms such as entry prevention, ROS buildup, budding and creation of a negative RNA strand by CCM-C-dots	93
Glycyrrhizic acid	Respiratory syndrome virus (PRRSV)	Gly-C-dots may primarily hinder PRRSV invasion and replication to suppress it	94
PEG-diamine with ascorbic acid	RNA viruses like porcine reproductive and respiratory disease viruses	Prevent RNA viruses replication	95

centrifugation and dialyzed. It was discovered that the CCM-C-dots prevented virus entry, creation of the negative strand of RNA, and budding. It was revealed that viral replication suppression is due to interferon-stimulating gene stimuli, pro-inflammatory cytokine formation, and accumulation of ROS. C-dots have demonstrated their ability to be inhibitors on a multisite level against the enteric coronavirus. The pyrolysis of curcumin yielded these hydrophilic, positively charged, 1.5 nm-sized antiviral fluorescent CCM-C-dots that are very effective against coronavirus models (porcine epidemic diarrhea virus).<sup>93</sup>

In 2020, Tong et al. found that respiratory syndrome virus (PRRSV) is suppressed by Gly-C-dots produced from glycyrrhizic acid and observed that Gly-C-dots possess a high level of antiviral activity on this specific virus. In conclusion, it was dictated that Gly-C-dot is not an effective preventer of either adsorption or release of PRRSV progeny when effects on viral proliferation were studied, focusing on stages of adsorption, invasion, replication, and release. Gly-C-dots may primarily hinder PRRSV invasion and replication to suppress it.<sup>94</sup> According to Dong et al., C-dots are successful replication inhibitors in RNA viruses such as porcine reproductive and respiratory disease viruses. A hydrothermal reaction must be carried out in a Teflon-coated autoclave chamber to yield C-dots from PEG-diamine and ascorbic acid. In vitro examination was done for antiviral activity against porcine reproductive and respiratory syndrome virus strain WUH3 in infected monkey kidney cells. Increased interferon production and upregulated interferon-stimulating gene expression prevent viral replication.<sup>95</sup> Despite the fact that these activities have been shown to be efficient antiviral mechanisms of C-dots, the precise method of action has never been specified and has remained unclear up to this point. In order to effectively inactivate and eliminate viruses using C-dots, it is required to investigate the specific method (Table 2).

**Anticancer Activity of C-dots.** Cancer is the second biggest cause of mortality globally, after cardiovascular disease.<sup>64</sup> Around 20 million new cases and 10 million fatalities from cancer were reported as of 2020, making cancer one of the deadliest diseases in the world. By 2030, the Global Cancer Observatory (GCO) predicts that 30 million people worldwide will die from cancer each year.<sup>96</sup> Cancer is characterized by abnormalities in cell cycle control mechanisms, which promote the survival and growth of malignant

cancer cells. Usually, when cancer develops, the signaling pathways are changed. The development of cancer and resistance to chemotherapy and radiotherapy are both influenced by the inhibition of physiological apoptosis.<sup>97</sup> Additionally, inflammation and immune system issues are connected to cancer. The five malignancies with the highest prevalence rates are breast (11.6%), lung (11.4%), colorectal (10.0%), prostate (7.3%), and stomach cancer (5.6%).<sup>98</sup> Cancer still accounts for a major portion of mortality despite significant advancements in both diagnosis and treatment. However, as of now, the biggest challenges facing oncologists are determining the correct cancer type and the optimal pharmacological dose that would have the most therapeutic impact with the least number of side effects. Therefore, it is crucial to make efforts in the areas of cancer prevention, diagnosis, and therapy.<sup>99</sup> In this approach, the development of anticancer drugs based on nanotechnologies, such as C-dots, could be promising candidates for the new era of cancer research.

Tan et al. found that even at a high dosage of 20 mg mL<sup>-1</sup> the C-dots made from grilled fish have a low cytotoxicity and great biocompatibility toward mouse osteoblast cells (MC3T3-E1).<sup>100</sup> C-dots made from candle soot with various chemical groups for surface functionalization were found to have cytotoxic effects, according to Zboril et al. Even though negatively charged C-dots formed from candle soot do not enter the cell nucleus, in vitro cytotoxicity tests on mouse fibroblasts (NIH/3T3) show that they can disrupt the cell cycle (by arresting the G2/M phase) and induce a high level of oxidative stress. At a concentration of 100 μg mL<sup>-1</sup>, the positively charged C-dots functionalized with PEI considerably alter the cell cycle (by halting the G0/G1 and G2/M phases) by penetrating the nucleus of the cell.<sup>101</sup>

However, at concentrations as high as 300 g mL<sup>-1</sup>, the polyethylene glycol-functionalized neutral C-dots do not alter the cell morphology, indicating their superior biocompatibility. Additionally, it is discovered that the mouse fibroblast cell line is unaffected by the hydrophobic thin films of C-dots that have been exposed to blue light (470 nm) for 6 h NIH/3T3.<sup>102</sup> Yousaf et al. highlighted the potential of FGQ-dots in the treatment of amyloidosis by reporting that they can suppress the aggregation of human islet amyloid polypeptide (hIAPP) with a minimum amount of cytotoxicity. Because they have hydrophobic groups and a high charge density, FGQ-dots can

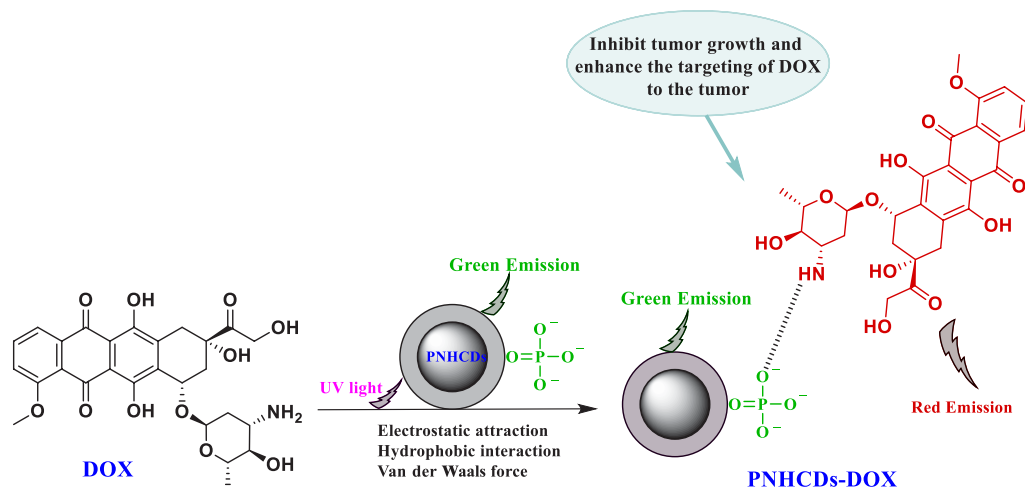


**Figure 6.** Preparation of nitrogen- and phosphorus-doped C-dots (PNHCds) loaded with DOX with tumors that were treated with PNHCds-DOX instead of free DOX.

attach to the hIAPP monomer and delay the aggregation process, as well as hinder the conformational change of hIAPP, which prevents the development of mature fibrils. Even at a high concentration of  $0.1 \text{ mg mL}^{-1}$ , red-fluorescent GQ-dots produced from *Mangifera indica* (mGQ-dots) with a size of 2–8 nm have been shown to be biocompatible with the mouse fibroblast cell line L929. Even though the biocompatibility of carbon nanomaterials has been established, the majority of the in vivo research used to assess cytotoxicity was conducted in vitro. These cytotoxicity studies do not meet the evaluation criteria for the clinical application of these nanoparticles because they lack trial data.<sup>103</sup> Because they are nontargeting and have unstable metabolic dynamics, conventional antitumor medications have low bioavailability and can harm normal cells. The bioavailability of antitumor medications must be increased immediately. The C-dots are endowed with EPR due to their natural, ultrasmall structure, which actively results in their aggregation at the tumor location. In addition to resolving the issue of drug targeting, using C-dots as carriers to transport antitumor medications to the body lengthens the period of time that the pharmaceuticals assemble at the tumor site.<sup>104</sup> Doxorubicin (DOX), an antitumor medication with a broad spectrum of activity, can prevent the synthesis of RNA and DNA, causing tumor cells in different growth cycles to die. By embedding and preventing the interface between DNA and polymer biosynthesis, DOX can impede DNA superhelix topoisomerase II, preventing replication of the DNA strand. Additionally, it has the ability to alter histones via activating transcription within the chromatin. DOX has been widely utilized in medical settings to treat a variety of illnesses, including breast cancer, lung cancer, ovarian cancer, leukemia, and stomach cancer.<sup>105</sup> As a result, it is now possible to incorporate DOX-loaded C-dots into the body to treat tumors. As depicted in Figure 6 the preparation of nitrogen- and phosphorus-doped C-dots (PNHCds) loaded with DOX involved heating glucose to boiling without further heating. When mice with tumors were treated with PNHCds-DOX instead of free DOX, the tumor volume in these mice was higher. However, the weight of the mice treated with PNHCds-DOX showed an upward trend, indicating that PNHCds-DOX could not only inhibit tumor growth but also enhance the targeting of DOX to the tumor, demonstrating the benefit of the EPR of C-dots. In contrast, the weight of the

tumor-bearing mice treated with free DOX gradually decreased.<sup>106</sup>

Additionally, Figure 7 depicts the schematic illustration of DOX-loaded and transferrin-modified C-dot-Trans-Dox show-

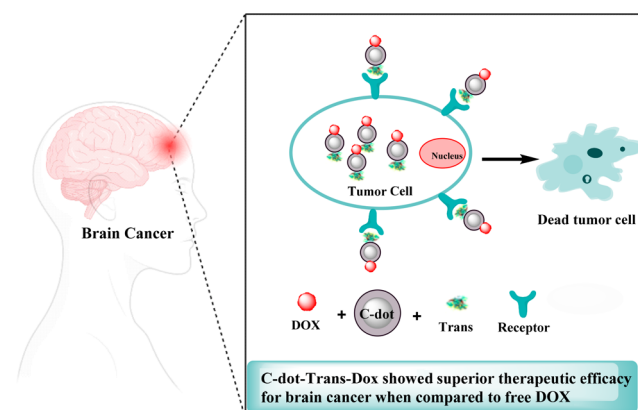


**Figure 7.** Schematic illustration for the multifunctional C-dot-Trans-Dox hybrid formed and the transferrin receptors present on both tumor cells and the BBB.

ing superior therapeutic efficacy for brain cancer when compared to free DOX. The ability of C-dot-Trans-Dox to cross the BBB and accumulate in brain tumor sites is made feasible by the transferrin receptors present on both tumor cells and the BBB. This finding holds promise for the future treatment of disorders associated with brain tumors. Furthermore, the CSCNP-R-CQDs' nitrogen functional groups on the surface allowed them to enter both the nuclei of cancer stem cells and tumor cells, opening up new avenues for the elimination of tumors. DOX is a pH-sensitive medication that is more soluble in acidic environments than in neutral ones. A suitable pH environment for the release of DOX can be provided by tumor tissues and cells, which also results in DOX being targeted at the tumor.<sup>107,108</sup>

The APCDs@Fe/DOX were created by Hou et al. by attaching modified aminoethyl anisamide (AEAA) to C-dots that had been loaded with DOX and Fe ions. After that, Losartan (Los) was wrapped in a mesoporous structure and attached to the other APCDs@Fe/DOX molecules by Asp-

Ala-thl-gly pro-Ala peptides (Pep), resulting in Pep-APCDs @ Fe/DOX-LOS. Fibroblast-activating protein (FAP) was toxic to Pep, but fibroblasts associated with cancer overexpressed FAP (CAFs). During the Pep-APCDs @Fe/DOX-LOS flow via the CAFs, Pep was degraded, while APCDs@Fe/DOX and Los were released. Los may reduce the tumor matrix because it alters the tumor microenvironment. Los, together with Fe ions and DOX, had the capacity to enhance the release of proinflammatory cytokines, expedite the infiltration of T cells and NK cells, and decrease the recruitment of immunosuppressive cells.<sup>109</sup>

When Kang et al. put silicon dioxide on a nanotube template's surface and raised the temperature, the silicon dioxide formed C-dots. The template concurrently disintegrated to create a hollow structure (C-hMOS), and the DOX was then soaked into the C-hMOS. Additionally, following heat treatment, the DOX-delivering C-hMOS displayed more notable fluorescence intensity, enabling them to study the dispersion of DOX in vivo.<sup>110</sup> Additionally, Türk et al. created the first pH-sensitive hydrogels by cross-linking hydroxyapatite, NCQDs, and DOX by themselves using Schiff bases, hydrogen bonds, and ion interactions. The Schiff base arrived at the tumor location and detached, releasing DOX.<sup>111</sup>

## ■ BIOCOMPATIBILITY AND TOXICITY OF C-DOTS

**Biocompatibility of C-dots.** Because C-dots enter the body and come into close contact with tissues and cells, evaluation of their biocompatibility is essential for biomedical applications. Blood compatibility C-dots are used as carriers for gene and drug delivery as well as biosensors upon direct blood contact. Hemagglutination, hemolysis, and coagulation behavior tests were used to evaluate the hemocompatibility of C-dots in vitro. The blood compatibility of materials can be determined with simplicity and precision via hemolysis.<sup>112</sup>

Li et al. investigated the hemocompatibility of fluorescent carbon dots made from  $\alpha$ -cyclodextrin by hydrothermal carbonization. Cellular and molecular levels of the carbon dots' impacts on the composition and functionality of important blood components were examined. They discovered that at concentrations of less than 0.1 mg/mL the carbon dots neither change the morphology of red blood cells nor induce lysis of red blood cells. Although the local fibrinogen microenvironment was disrupted by carbon dots at concentrations as high as 0.2 mg/mL, the secondary fibrinogen structure was only marginally affected. Up to 1 mg/mL of carbon dots in blood plasma did not significantly activate complement. The in vitro APTT and PT results were not significantly affected by the carbon dots at 0.1 mg/mL in blood plasma, and the in vitro whole blood coagulation was not adversely affected by 1 mg/mL of carbon dots. Platelet activators are typically present only in low concentrations of carbon dots. At concentrations as high as 50 mg/kg, the intravenous delivery of carbon dots did not compromise blood coagulation function. These results offer crucial information for avoiding potential risks and advancing the use of fluorescent carbon dots in medical applications.<sup>113</sup>

Zhong and co-workers created N,S-doped carbon dots (N,S-C-dots) in green fluorescent form using an easy one-step process. According to the TEM image, N,S-C-dots had homogeneous particle size and excellent dispersibility in solutions. The quantum yield (37.2%) was high for the N and S-C-dots in the meantime. Both flow analysis and confocal imaging demonstrated that N,S-C-dots could be

effectively absorbed by human umbilical vein endothelial cells (HUVECs) and localized in the cytoplasm of HUVECs. In vitro, N,S-C-dots exhibited nearly no cytotoxicity to HUVECs. Additionally, hemolysis rates resulting from different levels of N,S-C-dots were less than 0.5%. When N S-C-dots were administered, the erythrocyte morphology remained unchanged, and there was no accumulation, showing that N,S-C-dots had good blood compatibility. For in vivo imaging, the N,S-C-dots have an excellent future.<sup>114</sup>

The goal of the majority of the research is to determine whether foreign materials are compatible with human blood. These investigations revealed that the blood compatibility of these materials is influenced by different surface features. Biochemical characteristics such as surface area, surface charge, hydrophobicity/hydrophilicity, and so on influence how blood reacts to a substance when it comes into contact with it. In regard to C-dots, the variables that determine these reactions are surface, size effect, and structure.<sup>115</sup>

## ■ TOXICITY OF C-DOTS

**Evaluation.** C-dots have a great deal of potential in a variety of bioapplications because of their special optical qualities, broad surface area, and surface functionality. Biosafety concerns of C-dots have progressively come to light, as potential industrial and biological uses have been investigated. The toxicity profile of C-dots must be evaluated because of a higher probability that they will be used on humans. To assess the toxicity of C-dots, there are two primary approaches. There are in vitro and in vivo techniques for assessing the toxicity of C-dots. In vitro evaluation is one test that often involves measuring cell viability using assays like MTT, CCK-8, WST-1, and so on.<sup>116</sup> The experimental and control groups, respectively, are cells that have been cultivated with or without C-dots. Then, by comparison of these two groups, the toxicity of C-dots can be evaluated. A second blank group connected to the external environment is typically added in these experiments in order to remove the influence of the culture dish and selected tests.<sup>117</sup> Zhang et al. reported that tests like MTT or WST-1, which expose cultured cells to C-dots and measure cell viability by comparing it to the naive group and positive control, are commonly employed for in vitro approaches.<sup>118</sup>

Another type is known as an in vivo assessment, where a C-dot solution is injected directly into the bodies of organisms such as mice and zebrafish, either through a vein or the tail.<sup>112</sup> The toxicity and distribution of carboxylated C-dots in mice were initially investigated by Lee et al. Blood biochemical, hematological, and inflammatory analyses directed toward the liver, kidney, spleen, heart, or lung were carried out for a specific amount of time following delivery. Findings demonstrated that C-dots had no negative influence on living things or bodily tissues. Fluorescence imaging can be used to investigate how C-dots move through the body, first entering the bloodstream, then going via the spleen and kidneys, and ultimately leaving the body through the kidney filtration system.<sup>119</sup>

**Factors.** According to most publications on toxicity research, C-dots are either completely nontoxic or have very low toxicity. Nonetheless, the physicochemical characteristics of each C-dot as well as extrinsic parameters like surface charge, photolysis, concentration, etc., are all strongly correlated with the toxicity of C-dots. The distinct qualities that each type of C-dot carries ultimately dictate its level of

toxicity. Among these, the primary factor contributing to C-dot toxicity is a positive surface charge.<sup>120</sup>

According to further research, higher surface charge density significantly increases oxidative stress, IL-8 release, and mitochondrial malfunction, which can lead to allergic reactions or airway inflammation.<sup>121</sup> In one of the in vitro investigations, reactive red 2 (RR2), a raw material used to make C-dots, was tested for toxicity by using HeLa cells. Regarding the findings, C-dots made from RR2 had 70% higher cell survival than RR2, which was their progenitor. The preclinical safety of C-dots was further validated by in vivo tests conducted on zebra fish, which revealed decreased cytotoxicity.<sup>122</sup> Furthermore, the C-dots were radiolabeled in order to assess their biological distribution in animals. The results showed that C-dots were excreted by the kidney and feces.<sup>123</sup>

Liu et al. examined the biological distribution of C-dots in vivo for mammals for the first time using a radiolabeling technique. The findings show that C-dots are excreted from mice gradually through the kidney and feces and that there are no discernible harmful effects of C-dots on mice.<sup>124</sup> The effects of various injection routes on blood circulation, biodistribution, urine clearance, and passive tumor absorption by C-dots were investigated by Wu et al. Research has indicated that C-dots can be efficiently and rapidly eliminated from the body through the urine following any of the three injection techniques.<sup>125</sup> C-dots are a good option for bioapplications due to their quick elimination and low toxicity. This indicates that there is little in vivo toxicity and that C-dots do not accumulate.

## CONCLUSION AND FUTURE OUTLOOK

In this review, we mainly focus on the latest progress in the structure and synthesis of C-dots and their applications, which is particularly relevant for antimicrobial, antiviral, and anticancer activities. Various synthesis pathways have been thoroughly reviewed, and there are significant advantages such as low synthesis cost, ease of availability, and the fact that they can be produced on a large scale. The synthesized C-dots possess a wide range of significant advantages, including low cytotoxicity, efficiency for use in biosensors, in vitro bioimaging, drug delivery, and photocatalysis. Although these challenging actions are still being carried out on a persistent basis, significant progress has already been achieved in the field of C-dots. In terms of fundamental research and practical applications, the future of C-dots provides a good vision. Visible/natural activated antimicrobial compounds emerged as C-dots. The C-dots platform's remarkable potential in the killing/inhibition of bacteria, fungi, and viruses, including some multidrug-resistant species, has been established in several published studies, as has the road toward theranostics applications, as noted in this review. Extensive ongoing and new work on the further development and study of the C-dots platform, as well as on the mechanistic understanding of antimicrobial activity, might lead to rapid and significant advancements in fundamental research and technological applications.

## ASSOCIATED CONTENT

### Supporting Information

The Supporting Information is available free of charge at <https://pubs.acs.org/doi/10.1021/acsomega.3c05537>.

Diagram highlighting the research article identification and selection process based on inclusion and exclusion criteria (PDF)

## AUTHOR INFORMATION

### Corresponding Author

**Aso Hameed Hasan** – Department of Chemistry, Faculty of Science, Universiti Teknologi Malaysia, 81310 Johor Bahru, Johor, Malaysia; Department of Chemistry, College of Science, University of Garmian, Kalar 46021 Kurdistan Region, Iraq; [orcid.org/0000-0002-8375-1664](https://orcid.org/0000-0002-8375-1664); Email: [hhaso2@graduate.utm.my](mailto:hhaso2@graduate.utm.my), [aso.hameed@garmian.edu.krd](mailto:aso.hameed@garmian.edu.krd)

### Authors

**Narmin Hamaamin Hussien** – Department of Pharmacognosy and Pharmaceutical Chemistry, College of Pharmacy, University of Sulaimani, Sulaimani 46001, Iraq

**Yar Muhammed FaqiKhedr** – Department of Pharmacognosy and Pharmaceutical Chemistry, College of Pharmacy, University of Sulaimani, Sulaimani 46001, Iraq

**Andrey Bogoyavlenskiy** – Research and Production Center for Microbiology and Virology, Almaty 050010, Kazakhstan; [orcid.org/0000-0001-9579-2298](https://orcid.org/0000-0001-9579-2298)

**Ajmal R. Bhat** – Department of Chemistry, RTM Nagpur University, Nagpur 440033, India

**Joazaizulfazli Jamalis** – Department of Chemistry, Faculty of Science, Universiti Teknologi Malaysia, 81310 Johor Bahru, Johor, Malaysia

Complete contact information is available at:

<https://pubs.acs.org/10.1021/acsomega.3c05537>

### Notes

The authors declare no competing financial interest.

## ACKNOWLEDGMENTS

This work was supported by the Ministry of Education and Science of the Republic of Kazakhstan (grant no. BR10965178 “Development of original domestic drugs with antiviral activity efficient against COVID-19 and influenza” of Ministry of Education and Science of the Republic of Kazakhstan (Andrey Bogoyavlenskiy from Almaty, Kazakhstan)). The authors wish to thank Universiti Teknologi Malaysia and the Ministry of Higher Education (MOHE) Malaysia for funding this research under the Fundamental Research Grant Scheme (FRGS/1/2022/STG04/UTM/02/4).

## LIST OF ABBREVIATIONS

AFM, Atomic force microscopy  
BBB, Blood–brain barrier  
C-dots, Carbon dots  
CN-dots, Carbon nanodots  
CQ-dots, Carbon quantum dots  
CP-dots, Carbonized polymer dots  
DOX, Doxorubicin  
DLS, Dynamic light scattering  
VRE, *Enterococcus faecalis*  
EDA, Ethylenediamine  
GCO, Global Cancer Observatory  
GQ-dots, Graphene quantum dots  
HSV type 1, Herpes simplex virus type 1  
HIAPP, Human islet amyloid polypeptide

HRTEM, High-resolution transmission electron microscopy  
MRSA, Methicillin-resistant *Staphylococcus aureus*  
MIC, Minimum inhibitory concentration  
MDR, Multidrug resistant  
PL, Photoluminescence  
QY, Quantum yield  
ROS, Reactive oxygen species  
PRRSV, Respiratory syndrome virus  
SARS-CoV-2, Severe acute respiratory syndrome coronavirus 2  
TEM, Transmission electron microscope  
CDC, United States Centers for Disease Control and Prevention  
WSSV, White Spot Syndrome Virus

## REFERENCES

- (1) Xu, X.; Ray, R.; Gu, Y.; Ploehn, H. J.; Gearheart, L.; Raker, K.; Scrivens, W. A. Electrophoretic Analysis and Purification of Fluorescent Single-Walled Carbon Nanotube Fragments. *J. Am. Chem. Soc.* **2004**, *126* (40), 12736–12737.
- (2) Sun, Y.-P.; Zhou, B.; Lin, Y.; Wang, W.; Fernando, K. A. S.; Pathak, P.; Mezzani, M. J.; Harruff, B. A.; Wang, X.; Wang, H.; Luo, P. G.; Yang, H.; Kose, M. E.; Chen, B.; Veca, L. M.; Xie, S.-Y.; et al. Quantum-Sized Carbon Dots for Bright and Colorful Photoluminescence. *J. Am. Chem. Soc.* **2006**, *128* (24), 7756–7757.
- (3) Jing, H.; Bardakci, F.; Akgol, S.; Kusat, K.; Adnan, M.; Alam, M.; Gupta, R.; Sahreen, S.; Chen, Y.; Gopinath, S.; Sasidharan, S. Green Carbon Dots: Synthesis, Characterization, Properties and Biomedical Applications. *J. Funct. Biomater.* **2023**, *14*, 27.
- (4) Fernando, K. A. S.; Sahu, S.; Liu, Y.; Lewis, W. K.; Guliant, E. A.; Jafariyan, A.; et al. Carbon quantum dots and applications in photocatalytic energy conversion. *ACS Appl. Mater. Interfaces* **2015**, *7*, 8363–76.
- (5) Roy, P.; Chen, P. C.; Periasamy, A. P.; Chen, Y. N.; Chang, H. T. Photoluminescent carbon nanodots: synthesis, physicochemical properties and analytical applications. *Mater. Today* **2015**, *18*, No. 447.
- (6) Mohammed, S. J.; Omer, K. M.; Hawaiz, F. E. Deep insights to explain the mechanism of carbon dot formation at various reaction times using the hydrothermal technique: FT-IR, <sup>13</sup>C-NMR, <sup>1</sup>H-NMR, and UV-visible spectroscopic approaches. *RSC Adv.* **2023**, *13*, 14340–14349.
- (7) Calabrese, G.; De Luca, G.; Nocito, G.; Rizzo, M. G.; Lombardo, S. P.; Chisari, G.; Forte, S.; Sciuto, E. L.; Conoci, S. Carbon Dots: An Innovative Tool for Drug Delivery in Brain Tumors. *Int. J. Mol. Sci.* **2021**, *22* (21), 11783.
- (8) Ross, S.; Wu, R.-S.; Wei, S.-C.; Ross, G. M.; Chang, H.-T. The analytical and biomedical applications of carbon dots and their future theranostic potential: A review. *Journal of food and drug analysis* **2020**, *28* (4), No. 678.
- (9) Mansuriya, B. D.; Altintas, Z. Carbon Dots: Classification, Properties, Synthesis, Characterization, and Applications in Health Care—An Updated Review (2018–2021). *Nanomaterials* **2021**, *11*, 2525.
- (10) Adam, G. O.; Sharker, S. M.; Ryu, J. H. Emerging Biomedical Applications of Carbon Dot and Polymer Composite Materials. *Appl. Sci.* **2022**, *12*, 10565.
- (11) Sharma, S.; Umar, A.; Sood, S.; Mehta, S. K.; Kansal, S. K. Photoluminescent C-dots: An overview on the recent development in the synthesis, physicochemical properties and potential applications. *J. Alloys Compd.* **2018**, *748*, 818–853.
- (12) Khan, M. E.; Mohammad, A.; Yoon, T. State-of-the-art developments in carbon quantum dots (CQDs): Photo-catalysis, bio-imaging, and bio-sensing applications. *Chemosphere* **2022**, *302*, No. 134815.
- (13) Rao, N.; Singh, R.; Bashambu, L. Carbon-based nanomaterials: Synthesis and prospective applications. *Materials Today: Proceeding* **2021**, *44*, 608–614.
- (14) Jorns, M.; Pappas, D. A Review of Fluorescent Carbon Dots, Their Synthesis, Physical and Chemical Characteristics, and Applications. *Nanomaterials* **2021**, *11*, 1448.
- (15) Zhang, R.; Chen, A.; Yu, Y.; Chai, Y.; Zhuo, Y.; Yuan, R. Electrochemiluminescent carbon dot-based determination of micro-RNA-21 by using a hemin/G-wire supramolecular nanostructure as co-reaction accelerator. *Microchimica Acta* **2018**, *185*, 432.
- (16) Chae, A.; Choi, Y.; Jo, S.; Nur'aeni, N.'a.; Paoprasert, P.; Park, S. Y.; In, I. Microwave-assisted synthesis of fluorescent carbon quantum dots from an A2/B3 monomer set. *RSC Adv.* **2017**, *7*, 12663–12669.
- (17) Rigodanza, F.; Dorđević, L.; Arcudi, F.; Prato, M. Customizing the Electrochemical Properties of Carbon Nanodots by Using Quinones in Bottom-Up Synthesis. *Angew. Chem., Int. Ed. Engl.* **2018**, *57* (18), 5062–5067.
- (18) Yang, X.; Wan, Y.; Zheng, Y.; He, F.; Yu, Z.; Huang, J.; Wang, H.; Ok, Y. S.; Jiang, Y.; Gao, B. Surface functional groups of carbon-based adsorbents and their roles in the removal of heavy metals from aqueous solutions: A critical review. *Chem. Eng. J.* **2019**, *366*, 608–621.
- (19) Wang, B.; Cai, H.; Waterhouse, G. I. N.; Qu, X.; Yang, B.; Lu, S. Carbon Dots in Bioimaging, Biosensing and Therapeutics: A Comprehensive Review. *Small Sci.* **2022**, *2*, No. 2200012.
- (20) Fawaz, W.; Hasian, J.; Alghoraibi, I. Synthesis and physicochemical characterization of carbon quantum dots produced from folic acid. *Sci. Rep.* **2023**, *13*, x.
- (21) Jorns, M.; Pappas, D. A Review of Fluorescent Carbon Dots, Their Synthesis, Physical and Chemical Characteristics, and Applications. *Nanomaterials* **2021**, *11* (6), 1448.
- (22) Wang, Y.; Hu, A. Carbon quantum dots: synthesis, properties and applications. *J. Mater. Chem. C* **2014**, *2*, 6921.
- (23) Yadav, P. K.; Chandra, S.; Kumar, V.; Kumar, D.; Hasan, S. H. Carbon Quantum Dots: Synthesis, Structure, Properties, and Catalytic Applications for Organic Synthesis. *Catalysts* **2023**, *13* (2), 422.
- (24) Chae, A.; Choi, Y.; Jo, S.; Nur'aeni, N.'a.; Paoprasert, P.; Park, S. Y.; In, I. Microwave-assisted synthesis of fluorescent carbon quantum dots from an A2/B3 monomer set. *RSC Adv.* **2017**, *7* (21), 12663.
- (25) Liu, J.; Li, R.; Yang, B. Carbon Dots: A New Type of Carbon-Based Nanomaterial with Wide Applications. *ACS Cent. Sci.* **2020**, *6* (12), 2179–2195.
- (26) Koutsogiannis, P.; Thomou, E.; Stamatis, H.; Gournis, D.; Rudolf, P.; et al. Advances in fluorescent carbon dots for biomedical applications. *Adv. Phys.* **2020**, *5* (1), No. 1758592.
- (27) Campuzano, S.; Yanez-Sedeno, P.; Pingarron, J. M. Carbon Dots and Graphene Quantum Dots in Electrochemical Biosensing. *Nanomaterials* **2019**, *9* (4), 634.
- (28) Xia, C.; Zhu, S.; Feng, T.; Yang, M.; Yang, B. Evolution and Synthesis of Carbon Dots: From Carbon Dots to Carbonized Polymer Dots. *Adv. Sci.* **2019**, *6*, No. 1901316.
- (29) Zhou, Y.; Sharma, S.; Peng, Z.; Leblanc, R. Polymers in Carbon Dots: A Review. *Polymers* **2017**, *9* (2), 67.
- (30) Sharker, S. M.; Do, M. Nanoscale Carbon-Polymer Dots for Theranostics and Biomedical Exploration. *J. Nanotheranostics* **2021**, *2*, 118–130.
- (31) Cui, L.; Ren, X.; Sun, M.; Liu, H.; Xia, L. Carbon Dots: Synthesis, Properties and Applications. *Nanomaterials (Basel)* **2021**, *11* (12), 3419.
- (32) Hawrylak, P.; Peeters, F.; Ensslin, K. Carbononics—Integrating electronics, photonics and spintronics with graphene quantum dots. *Phys. Status Solidi RRL* **2016**, *10*, 11–12.
- (33) Hai, K.; Feng, J.; Chen, X. W.; Wang, J. H. Tuning the optical properties of graphene quantum dots for biosensing and bioimaging. *J. Mater. Chem. B* **2018**, *6*, 3219–3234.
- (34) Seliverstova, E.; Ibrayev, N.; Menshova, E. Modification of structure and optical properties of graphene oxide dots, prepared by

- laser ablation method. *Fuller. Nanotub. Carbon Nanostruct.* **2022**, *30*, 119.
- (35) Yao, Y. Y.; Gedda, G.; Girma, W. M.; Yen, C. L.; Ling, Y. C.; Chang, J. Y. Magnetofluorescent carbon dots derived from crab shell for targeted dual-modality bioimaging and drug delivery. *ACS Appl. Mater. Interfaces.* **2017**, *9*, 13887–13899.
- (36) Kumawat, M. K.; Thakur, M.; Gurung, R. B.; Srivastava, R. Graphene quantum dots from mangifera indica: Application in near-infrared bioimaging and intracellular nanothermometry. *ACS Sustain. Chem. Eng.* **2017**, *5*, 1382–1391.
- (37) Pires, N. R.; Santos, C. M. W.; Sousa, R. R.; Paula, R. C. M. d.; Cunha, P. L. R.; Feitosa, J. P. A. Novel and Fast Microwave-Assisted Synthesis of Carbon Quantum Dots from Raw Cashew Gum. *J. Brazil. Chem. Soc.* **2015**, *26*, 1274–1282.
- (38) Magesh, V.; Sundramoorthy, A. K.; Ganapathy, D. Recent Advances on Synthesis and Potential Applications of Carbon Quantum Dots. *Front. Mater.* **2022**, *9*, x.
- (39) Kang, S.; Mhin, S.; Han, H.; Kim, K.; Jones, J. L.; Ryu, J. H.; Kang, J. S.; Kim, S. H.; Shim, K. B. Ultrafast Method for Selective Design of Graphene Quantum Dots with Highly Efficient Blue Emission. *Sci. Rep.* **2016**, *6*, 38423.
- (40) Ren, X.; Zhang, F.; Guo, B. P.; Gao, N.; Zhang, X. L. Synthesis of N-Doped Micropore Carbon Quantum Dots with High Quantum Yield and Dual-Wavelength Photoluminescence Emission from Biomass for Cellular Imaging. *Nanomaterials* **2019**, *9*, 495.
- (41) Cui, L.; Ren, X.; Wang, J. G.; Sun, M. T. Synthesis of homogeneous carbon quantum dots by ultrafast dual-beam pulsed laser ablation for bioimaging. *Mater. Today Nano* **2020**, *12*, 100091.
- (42) Zhao, P.; Yang, M.; Fan, W.; Wang, X.; Tang, F.; Yang, C.; Dou, X.; Li, S.; Wang, Y.; Cao, Y. Facile one-pot conversion of petroleum asphaltene to high quality green fluorescent graphene quantum dots and their application in cell imaging. *Part. Syst. Character.* **2016**, *33*, 635–644.
- (43) Gunjal, D. B.; Gurav, Y. M.; Gore, A. H.; Naik, V. M.; Waghmare, R. D.; Patil, C. S.; Sohn, D.; Anbhule, P. V.; Shejwal, R. V.; Kolekar, G. B. Nitrogen doped waste tea residue derived carbon dots for selective quantification of tetracycline in urine and pharmaceutical samples and yeast cell imaging application. *Opt. Mater.* **2019**, *98*, No. 109484.
- (44) Zhao, S.; Lan, M.; Zhu, X.; Xue, H.; Ng, T. W.; Meng, X.; Lee, C. S.; Wang, P.; Zhang, W. Green synthesis of bifunctional fluorescent carbon dots from garlic for cellular imaging and free radical scavenging. *ACS Appl. Mater. Interfaces* **2015**, *7*, 17054–17060.
- (45) Zhao, Y.; Wu, X.; Sun, S.; Ma, L.; Zhang, L.; Lin, H. A facile and highefficient approach to yellow emissive graphene quantum dots from grapheme oxide. *Carbon.* **2017**, *124*, 342–347.
- (46) Ma, C.; Zhu, Z.; Wang, H.; Huang, X.; Zhang, X.; Qi, X.; Zhang, H. L.; Zhu, Y.; Deng, X.; Peng, Y.; et al. A General Solid-State Synthesis of Chemically-Doped Fluorescent Graphene Quantum Dots for Bioimaging and Optoelectronic Applications. *Nanoscale* **2015**, *7*, 10162–10169.
- (47) Praneeraj, J.; Neungnoraj, K.; In, I.; Paoprasert, P. Environmentally friendly supercapacitor based on carbon dots from durian peel as an electrode. *Key Eng. Mater.* **2019**, *803*, 115–119.
- (48) Tian, R.; Zhong, S.; Wu, J.; Jiang, W.; Shen, Y.; Jiang, W.; Wang, T. Solvothermal method to prepare graphene quantum dots by hydrogen peroxide. *Opt. Mater.* **2016**, *60*, 204–208.
- (49) Liu, W.; Diao, H.; Chang, H.; Wang, H.; Li, T.; Wei, W. Green synthesis of carbon dots from rose-heart radish and application for Fe<sup>3+</sup> detection and cell imaging. *Sens. Actuators B Chem.* **2017**, *241*, 190–198.
- (50) Huang, K.; Lu, W.; Yu, X.; Jin, C.; Yang, D. Highly pure and luminescent graphene quantum dots on silicon directly grown by chemical vapor deposition. *Part. Part. Syst. Character.* **2016**, *33*, 8–14.
- (51) Kumar, S.; Aziz, S.; Girshevitz, O.; Nessim, G. One-step synthesis of N-doped graphene quantum dots from chitosan as a sole precursor using chemical vapor deposition. *J. Phys. Chem. C* **2018**, *122*, 2343–2349.
- (52) Hussien, N. H.; Hamid, S. J.; Sabir, M. N.; Hasan, A. H.; Mohammed, S. J.; Shali, A. A.K. Novel Penicillin Derivatives Against Selected Multiple-Drug Resistant Bacterial Strains: Design, Synthesis, Structural Analysis, in silico and in Vitro Studies. *Current Organic Synthesis* **2023**, DOI: 10.2174/1570179420666230510104319.
- (53) Salih, R. H. H.; Hasan, A. H.; Hussien, N. H.; Hawaiz, F. E.; Hadda, T. B.; Jamal, J.; Almalki, F. A.; Adeyinka, A. S.; Coetzee, L.-C. C.; Oyebamiji, A. K. Thiazole-pyrazoline hybrids as potential antimicrobial agent: Synthesis, biological evaluation, molecular docking, DFT studies and POM analysis. *J. Mol. Struct.* **2023**, *1282*, No. 135191.
- (54) Hussien, N. H. A.; Qadir, S. H.; Rahman, H. S.; Hamalaw, Y. Y.; Kareem, P. S. S.; Hamza, B. A.; et al. Long-term toxicity of fluoroquinolones: a comprehensive review. *Drug and Chemical Toxicology* **2023**, *46* (4), 1–12.
- (55) Adamski, P.; Byczkowska-Rostkowska, Z.; Gajewska, J.; Zakrzewski, A. J.; Klebukowska, L. Prevalence and Antibiotic Resistance of Bacillus sp. Isolated from Raw Milk. *Microorganisms* **2023**, *11*, 1065.
- (56) Qamar, F. N.; Yousafzai, M.T.; Dehraj, I. F.; Shakoor, S.; Irfan, S.; et al. Antimicrobial Resistance in Typhoidal Salmonella: Surveillance for Enteric Fever in Asia Project, 2016–2019. *Clin Infect Dis.* **2020**, *71*, S276–S284.
- (57) Morris, S.; Cerceo, E. Trends, Epidemiology, and Management of Multi-Drug Resistant Gram-Negative Bacterial Infections in the Hospitalized Setting. *Antibiotics (Basel)* **2020**, *9* (4), 196.
- (58) Dadgostar, P. Antimicrobial Resistance: Implications and Costs. *Infect Drug Resist.* **2019**, *12*, 3903–3910.
- (59) de Kraker, M. E. A.; Stewardson, A. J.; Harbarth, S. Will 10 Million People Die a Year due to Antimicrobial Resistance by 2050? *PLoS Med.* **2016**, *13* (11), No. e1002184.
- (60) Vaou, N.; Stavropoulou, E.; Voidarou, C.; Tsigalou, C.; Bezirtzoglou, E. Towards Advances in Medicinal Plant Antimicrobial Activity: A Review Study on Challenges and Future Perspectives. *Microorganisms* **2021**, *9* (10), 2041.
- (61) Wang, L.; Hu, C.; Shao, L. The antimicrobial activity of nanoparticles: present situation and prospects for the future. *Int. J. Nanomedicine* **2017**, *12*, 1227–1249.
- (62) Sharmin, S.; Rahaman, M. M.; Sarkar, C.; Atolani, O.; Islam, M. T.; Adeyemi, O. S. Nanoparticles as antimicrobial and antiviral agents: A literature-based perspective study. *Heliyon.* **2021**, *7* (3), No. e06456.
- (63) Dong, X.; Liang, W.; Mezziani, M. J.; Sun, Y.-P.; Yang, L. Carbon Dots as Potent Antimicrobial Agents. *Theranostics* **2020**, *10* (2), 671–686.
- (64) Jhonsi, M. A.; Ananth, D. A.; Nambirajan, G.; Sivasudha, T.; Yamini, R.; Bera, S.; et al. antimicrobial activity, cytotoxicity and DNA binding studies of carbon dots. *Spectrochim Acta A* **2018**, *196*, 295–302.
- (65) Hussien, N. H.; Hasan, A. H.; Muhammed, G. O.; Yassin, A. Y.; Salih, R. R.; Esmail, P. A.; Alanazi, M. M.; Jamal, J. Anthracycline in Medicinal Chemistry: Mechanism of Cardiotoxicity, Preventive and Treatment Strategies. *Curr. Org. Chem.* **2023**, *27* (4), 363–377.
- (66) Su, L.-J.; Zhang, J.-H.; Gomez, H.; Murugan, R.; Hong, X.; Xu, D.; Jiang, F.; Peng, Z.-Y. Reactive Oxygen Species-Induced Lipid Peroxidation in Apoptosis, Autophagy, and Ferroptosis. *Oxid. Med. Cell Longev* **2019**, *2019*, No. 5080843.
- (67) Mezziani, M. J.; Dong, X.; Zhu, L.; Jones, L. P.; LeCroy, G. E.; Yang, F.; Wang, S.; Wang, P.; Zhao, Y.; Yang, L.; Tripp, R. A.; Sun, Y.-P. Visible Light-Activated Bactericidal Functions of Carbon "Quantum" Dots. *ACS Appl. Mater. Interfaces* **2016**, *8* (17), 10761.
- (68) Bing, W.; Sun, H.; Yan, Z.; Ren, J.; Qu, X.; et al. Programmed Bacteria Death Induced by Carbon Dots with Different Surface Charge. *Small* **2016**, *12*, 4713–4718.
- (69) Su, S.; Shelton, C. B.; Qiu, J.; et al. *Proceedings of the ASME 2013 International Mechanical Engineering Congress and Exposition*; California, USA, Nov. 2013.

- (70) Yang, J.; Zhang, X.; Ma, Y.-H.; Gao, G.; Chen, X.; Jia, H.-R.; Li, Y.-H.; Chen, Z.; Wu, F. G. *ACS Appl. Mater. Interfaces* **2016**, *8*, 32170–32181.
- (71) Li, H.; Huang, J.; Song, Y. X.; Zhang, M. L.; Wang, H. B.; Lu, F.; et al. Degradable Carbon Dots with Broad-Spectrum Antibacterial Activity. *ACS Appl. Mater. Inter.* **2018**, *10*, 26936–46.
- (72) Hou, P.; Yang, T.; Liu, H.; Li, Y. F.; Huang, C. Z. An active structure preservation method for developing functional graphitic carbon dots as an effective antibacterial agent and a sensitive pH and Al(III) nanosensor. *Nanoscale*. **2017**, *9*, 17334–41.
- (73) Sidhu, J. S.; et al. The Photochemical Degradation of Bacterial Cell Wall Using Penicillin-Based Carbon Dots: Weapons Against Multi-Drug Resistant (MDR) Strains. *Chemistryselect*. **2017**, *2*, 9277–83.
- (74) Liang, J.; Li, W.; Chen, J.; Huang, X.; Liu, Y.; Zhang, X.; Shu, W.; Lei, B.; Zhang, H. Antibacterial Activity and Synergetic Mechanism of Carbon Dots against Gram-Positive and -Negative Bacteria. *ACS Appl. Bio Mater.* **2021**, *4* (9), 6937.
- (75) Romero, M. P.; Alves, F.; Stringasci, M. D.; Buzza, H. H.; Ciol, H.; Inada, N. M.; Bagnato, V. S. One-Pot Microwave-Assisted Synthesis of Carbon Dots and in vivo and in vitro Antimicrobial Photodynamic Applications. *Front Microbiol.* **2021**, *12*, No. 662149.
- (76) Jian, H.-J.; Wu, R.-S.; Lin, T.-Y.; Li, Y.-J.; Lin, H.-J.; Harroun, S. G.; Lai, J.-Y.; Huang, C.-C. Super-Cationic Carbon Quantum Dots Synthesized from Spermidine as an Eye Drop Formulation for Topical Treatment of Bacterial Keratitis. *ACS Nano* **2017**, *11* (7), 6703–6716.
- (77) Chai, S.; Zhou, L.; Pei, S.; Zhu, Z.; Chen, B. P-Doped Carbon Quantum Dots with Antibacterial Activity. *Micromachines* **2021**, *12*, 1116.
- (78) Zhao, D.; Zhang, R.; Liu, X.; Li, X.; Xu, M.; Huang, X.; Xiao, X. Screening of Chitosan Derivatives-Carbon Dots Based on Antibacterial Activity and Application in Anti-Staphylococcus aureus Biofilm. *Int. J. Nanomed.* **2022**, *17*, 937–952.
- (79) Wu, L.; Gao, Y.; Zhao, C.; Huang, D.; Chen, W.; Lin, X.; Liu, A.; Lin, L. Synthesis of curcumin-quaternized carbon quantum dots with enhanced broad-spectrum antibacterial activity for promoting infected wound healing. *Biomater Adv.* **2022**, *133*, No. 112608.
- (80) Priyadarshini, E.; Rawat, K.; Prasad, T.; Bohidar, H. B. Antifungal efficacy of Au@ carbon dots nanoconjugates against opportunistic fungal pathogen, *Candida albicans*. *Colloid Surface B* **2018**, *163*, 355–61.
- (81) Jhonsi, M. A.; Ananth, D. A.; Nambirajan, G.; Sivasudha, T.; Yamini, R.; Bera, S.; et al. Antimicrobial activity, cytotoxicity and DNA binding studies of carbon dots. *Spectrochim Acta A* **2018**, *196*, 295–302.
- (82) Rispaill, N.; De Matteis, L.; Santos, R.; Miguel, A.S.; Custardoy, L.; et al. Quantum dots and superparamagnetic nanoparticle interaction with pathogenic fungi: internalization and toxicity profile. *ACS Appl. Mater. Interfaces* **2014**, *6* (12), 9100–9110.
- (83) Bagheri, Z.; Ehtesabi, H.; Hallaji, Z.; Aminoroaya, N.; Tavana, H.; Behroodi, E.; et al. On-chip analysis of carbon dots effect on yeast replicative lifespan. *Anal. Chim. Acta* **2018**, *1033*, 119–27.
- (84) Kaloyan, K.; Andonova-Lilova, B.; Smaghe, G. Inhibitory activity of carbon quantum dots against *Phytophthora infestans* and fungal plant pathogens and their effect on dsRNA-induced gene silencing. *Biotechnology & Biotechnological equipment* **2022**, *36* (1), 949–959.
- (85) Hamaamin Hussien, N.; Hameed Hasan, A.; Jamalis, J.; Shakya, S.; Chander, S.; Kharkwal, H.; Murugesan, S.; Ajit Bastikar, V.; Pyarelal Gupta, P. Potential inhibitory activity of phytoconstituents against black fungus: In silico ADMET, molecular docking and MD simulation studies. *Computational Toxicology*. **2022**, *24*, No. 100247.
- (86) Hasan, A. H.; Hussien, N. H.; Shakya, S.; Jamalis, J.; Pratama, M. R. F.; Chander, S.; Kharkwal, H.; Murugesan, S. In silico discovery of multi-targeting inhibitors for the COVID-19 treatment by molecular docking, molecular dynamics simulation studies, and ADMET predictions. *Structural Chemistry* **2022**, *33* (5), 1645–1665.
- (87) Amin Huseen, N. H. Docking study of naringin binding with COVID-19 main protease enzyme. *IJPS* **2020**, *29* (2), 231–238.
- (88) Rahman, H. S.; Abdulateef, D. S.; Hussien, N. H.; Salih, A. F.; Othman, H. H.; Mahmood Abdulla, T.; Omer, S. H. S.; Mohammed, T. H.; Mohammed, M. O.; Aziz, M. S.; Abdullah, R. Recent Advancements on COVID-19: A Comprehensive Review. *International journal of general medicine* **2021**, *14*, 10351.
- (89) Huang, S.; Gu, J.; Ye, J.; Fang, B.; Wan, S.; Wang, C.; Ashraf, U.; Li, Q.; Wang, X.; Shao, L.; Song, Y.; Zheng, X.; Cao, F.; Cao, S. Benzoxazine monomer derived carbon dots as a broad-spectrum agent to block viral infectivity. *J. Colloid Interface Sci.* **2019**, *542*, 198–206.
- (90) Huang, H.-T.; Lin, H.-J.; Huang, H.-J.; Huang, C.-C.; Lin, J. H.-Y.; Chen, L.-L. Synthesis and evaluation of polyamine carbon quantum dots (CQDs) in *Litopenaeus vannamei* as a therapeutic agent against WSSV. *Sci. Rep.* **2020**, *10*, 7343.
- (91) Garg, P.; Sangam, S.; Kochhar, D.; Pahari, S.; Kar, C.; Mukherjee, M. Exploring the role of triazole functionalized heteroatom co-doped carbon quantum dots against human coronaviruses. *Nano Today* **2020**, *35*, No. 101001.
- (92) Barras, A.; Pagneux, Q.; Sane, F.; Wang, Q.; Boukherroub, R.; Hober, D.; Szunerits, S. High Efficiency of Functional Carbon Nanodots as Entry Inhibitors of Herpes Simplex Virus Type 1. *ACS Appl. Mater. Interfaces* **2016**, *8* (14), 9004–13.
- (93) Kwee, Y.; Zhou, Y.; Fahmi, M. Z.; Sharon, M.; Kristanti, A. N. Progress on Applying Carbon Dots for Inhibition of RNAVirus Infection. *Nanotheranostics* **2022**, *6* (4), 436–450.
- (94) Tong, T.; Hu, H.; Zhou, J.; Deng, S.; Zhang, X.; Tang, W.; Fang, L.; Xiao, S.; Liang, J. Glycyrrhizic-Acid-Based Carbon Dots with High Antiviral Activity by Multisite Inhibition Mechanisms. *Small* **2020**, *16*, No. 1906206.
- (95) Dong, X.; Moyer, M. M.; Yang, F.; Sun, Y. P.; Yang, L. Carbon Dots' Antiviral Functions Against Noroviruses. *Sci. Rep.* **2017**, *7*, 519.
- (96) Nagai, H.; Kim, Y. H. Cancer prevention from the perspective of global cancer burden patterns. *J. Thorac Dis* **2017**, *9* (3), 448–451.
- (97) Otto, T.; Sicinski, P. Cell cycle proteins as promising targets in cancer therapy. *Nat. Rev. Cancer* **2017**, *17* (2), 93–115.
- (98) Sung, H.; Ferlay, J.; Siegel, R. L.; Laversanne, M.; Soerjomataram, I.; Jemal, A.; Bray, F.; et al. Global Cancer Statistics 2020: GLOBOCAN Estimates of Incidence and Mortality Worldwide for 36 Cancers in 185 Countries. *CA Cancer J. Clin* **2021**, *71*, 209–249.
- (99) Greten, F. R.; Grivennikov, S. I. Inflammation and Cancer: Triggers, Mechanisms and Consequences. *Immunity* **2019**, *51* (1), 27–41.
- (100) Bi, J.; Li, Y.; Wang, H.; Song, Y.; Cong, S.; Li, D.; Zhou, D.; Zhu, B.-W.; Tan, M. *New J. Chem.* **2017**, *41*, 8490–8496.
- (101) Havrdova, M.; Hola, K.; Skopalik, J.; Tomankova, K.; Petr, M.; Cepe, K.; Polakova, K.; Tucek, J.; Bourlinos, A. B.; Zboril, R. *Carbon* **2016**, *99*, 238–248.
- (102) Stankovic, N. K.; Bodik, M.; Siffalovic, P.; Kotlar, M.; Micusik, M.; Spitalsky, Z.; Danko, M.; Miliwojevic, D. D.; Kleinova, A.; Kubat, P.; Capakova, Z.; Humpolicek, P.; Lehocky, M.; Todorovic Markovic, B. M.; Markovic, Z. M. Antibacterial and Antibiofouling Properties of Light Triggered Fluorescent Hydrophobic Carbon Quantum Dots. *ACS Sustainable Chem. Eng.* **2018**, *6*, 4154–4163.
- (103) Yousaf, M.; Huang, H.; Li, P.; Wang, C.; Yang, Y. *ACS Chem. Neurosci.* **2017**, *8*, 1368–1377.
- (104) Anand, A.; Unnikrishnan, B.; Wei, S.-C.; Chou, C. P.; Zhang, L.-Z.; Huang, C.-C. Graphene oxide and carbon dots as broad-spectrum antimicrobial agents – a minireview. *Nanoscale Horiz.* **2019**, *4*, 117–137.
- (105) Kashyap, B. K.; Singh, V. V.; Solanki, M. K.; Kumar, A.; Ruokolainen, J.; Kesari, K. K. Smart Nanomaterials in Cancer Theranostics: Challenges and Opportunities. *ACS Omega* **2023**, *8*, 14290–14320.
- (106) Kciuk, M.; Gielecinska, A.; Mujwar, S.; Kolat, D.; Kaluzinska-Kolat, Z.; Celik, I.; Kontek, R. Doxorubicin—An Agent with Multiple Mechanisms of Anticancer Activity. *Cells* **2023**, *12* (4), 659.

- (107) Gong, X.; Zhang, Q.; Gao, Y.; Shuang, S.; Choi, M. M. F.; Dong, C. Phosphorus and Nitrogen Dual-Doped Hollow Carbon Dot as A Nanocarrier for Doxorubicin Delivery and Biological Imaging. *ACS Appl. Mater. Interfaces* **2016**, *8* (18), 11288.
- (108) Li, S.; Amat, D.; Peng, Z.; Vanni, S.; Raskin, S.; De Angulo, G.; Othman, A. M.; Graham, R. M.; Leblanc, R. M. Transferrin Conjugated Nontoxic Carbon Dots for Doxorubicin Delivery to Target Pediatric Brain Tumor Cells. *Nanoscale* **2016**, *8* (37), 16662.
- (109) Hou, L.; Chen, D.; Wang, R.; et al. Transformable honeycomb-like nanoassemblies of carbon dots for regulated multisite delivery and enhanced antitumor chemoimmunotherapy. *Angew. Chem., Int. Ed. Engl.* **2021**, *60* (12), 6581–6592.
- (110) Kang, S.; Kim, K. M.; Jung, K.; et al. Graphene oxide quantum dots derived from coal for bioimaging: facile and green approach. *Sci. Rep.* **2019**, *9* (1), 4101.
- (111) Turk, S.; Altınsoy, I.; Efe, G. C.; Ipek, M.; Ozacar, M.; Bindal, C. A novel multifunctional NCQDs-based injectable self-crosslinking and in situ forming hydrogel as an innovative stimuli responsive smart drug delivery system for cancer therapy. *Mater. Sci. Eng., C* **2021**, *121* (2021), x.
- (112) Singh, V.; Rawat, K. S.; Mishra, S.; Baghel, T.; Fatima, S.; John, A. A.; et al. Biocompatible fluorescent carbon quantum dots prepared from beetroot extract for in vivo live imaging in *C. elegans* and BALB/c mice. *J. Mater. Chem. B* **2018**, *6* (20), 3366–3371.
- (113) Li, S.; Guo, Z.; Zhang, Y.; Xue, W.; Liu, Z. Blood Compatibility Evaluations of Fluorescent Carbon Dots. *ACS Appl. Mater. Interfaces* **2015**, *7* (34), 19153–19162.
- (114) Zhong, J.; Chen, X.; Zhang, M.; Xiao, C.; Cai, L.; Khan, W. A.; Yu, K.; Cui, J.; He, L. Blood compatible heteroatom-doped carbon dots for bio-imaging of human umbilical vein endothelial cells. *Chin. Chem. Lett.* **2020**, *31* (3), 769–773.
- (115) Li, X.; Wang, L.; Fan, Y.; Feng, Q.; Cui, F.-z. Biocompatibility and Toxicity of Nanoparticles and Nanotubes. *J. Nanomater.* **2012**, *2012*, 1.
- (116) Wei, S.-M.; Feng, K.; Li, C.; Xie, N.; Wang, Y.; Yang, X.-L.; Chen, B.; Tung, C.-H.; Wu, L.-Z. ZnCl<sub>2</sub> Enabled Synthesis of Highly Crystalline and Emissive Carbon Dots with Exceptional Capability to Generate O<sub>2</sub>. *Matter* **2020**, *2*, 495–506.
- (117) Li; Wu, S.; Zhang, J.; Zhou, R.; Cai, X. Sulphur doped carbon dots enhance photodynamic therapy via PI3K/Akt signalling pathway. *Cell Proliferation* **2020**, *53*, No. e12821.
- (118) Zhang, M.; Zhai, X.; Ma, T.; Huang, Y.; Yan, C. H.; Du, Y. Multifunctional cerium doped carbon dots nanoplatfrom and its applications for wound healing. *Chem. Eng. J.* **2021**, *423*, No. 130301.
- (119) Nurunnabi, M.; Khatun, Z.; Huh, K. M.; Park, S. Y.; Lee, D. Y.; Cho, K. J.; Lee, Y.-k. In vivo biodistribution and toxicology of carboxylated graphene quantum dots. *ACS Nano* **2013**, *7* (8), 6858–67.
- (120) Wang, B.; Cai, H.; Waterhouse, G. I. N.; Qu, X.; Yang, B.; Lu, S. Carbon Dots in Bioimaging, Biosensing and Therapeutics: A Comprehensive Review. *Small Sci.* **2022**, *2*, No. 2200012.
- (121) Weiss, M.; Fan, J.; Claudel, M.; Sonntag, T.; Didier, P.; Ronzani, C.; et al. Density of surface charge is a more predictive factor of the toxicity of cationic carbon nanoparticles than zeta potential. *J. Nanobiotechnology* **2021**, *19* (1), 5.
- (122) Wang, B.; Cai, H.; Waterhouse, G. I. N.; Qu, X.; Yang, B.; Lu, S. Carbon dots in bioimaging, biosensing and therapeutics: A comprehensive review. *Small Sci.* **2022**, *2* (6), No. 2200012.
- (123) Kaurav, H.; Verma, D.; Bansal, A.; Kapoor, D. N.; Sheth, S. Progress in drug delivery and diagnostic applications of carbon dots: a systematic review. *Front. Chem.* **2023**, *11*, x.
- (124) Li, W.; Wu, S.; Zhang, H.; Zhang, X.; Zhuang, J.; Hu, C.; Liu, Y.; Lei, B.; Ma, L.; Wang, X. Enhanced Biological Photosynthetic Efficiency Using Light-Harvesting Engineering with Dual-Emissive Carbon Dots. *Adv. Funct. Mater.* **2018**, DOI: 10.1002/adfm.201804004.
- (125) Wu, J.; Lei, J. H.; He, B.; Deng, C.-X.; Tang, Z.; Qu, S. Generating long-wavelength absorption bands with enhanced deep red fluorescence and photothermal performance in fused carbon dots aggregates. *Aggregate.* **2021**, *2*, No. e139.